

6. CAE Analysis Results

6. CAE Analysis Results

6.1. Selected Tests for CAE

To verify that the ULSAB meets the targets set in the beginning of Phase 1, the following tests were chosen for the static and dynamic stiffness.

Structural Performances	Targets
Static torsion stiffness	$\geq 13000 \text{ Nm/deg}$
Static bending stiffness	$\geq 12200 \text{ N/mm}$
Normal modes (first modes)	$\geq 40 \text{ Hz}$

Figure 6.1-1 Load cases and targets for static and dynamic stiffness

For analytical crash testing the following tests were selected:

- AMS, 50% frontal offset crash at 55 km/h
- NCAP, 100% frontal crash at 35 mph (FMVSS 208)
- Side impact crash at 50 km/h (96/27 EG, with deformable barrier)
- Rear moving barrier crash at 35 mph (FMVSS 301)
- Roof crush (FMVSS 216)

6.2. Static and Dynamic Stiffness

Based on CAD surface data the FE-Model (Figure 6.2-1) for the body in white was created. Because of the structure symmetry, only a half model with certain boundary conditions at the symmetry plane at $y=0$ for the static and dynamic stiffness simulations were used. The stiffness model consists in triangle and quadrilateral elements. To connect the different structure components, different methods were used. To connect laser welded parts in the FE-Model, the nodes of the flanges were equivalent. For spot welded areas the middle flange nodes are connected with welding point elements. The weld point distance was with a point

distance of about 50 mm. The CAE configuration for the static and dynamic simulations consist of the following parts:

- Welded Body Structure
- Bonded Windshield and Back Light
- Bonded and bolted Panel Dash Insert (Part-No. 022)
- Bonded Panel Spare Tire Tub (Part-No. 050)
- Bolted Reinforcement Panel Dash Brake Booster (Part-No. 115)
- Bolted Braces Radiator (Part-No. 188)
- Bolted Reinforcement Radiator Rail Closeout RH/LH (Part -No. 094/095)
- Bolted Reinforcement Radiator Support Upper (Part-No. 001)
- Bolted Tunnel Bridge Lower/Upper
- Bolted Brace Cowl to Shock Tower Assembly

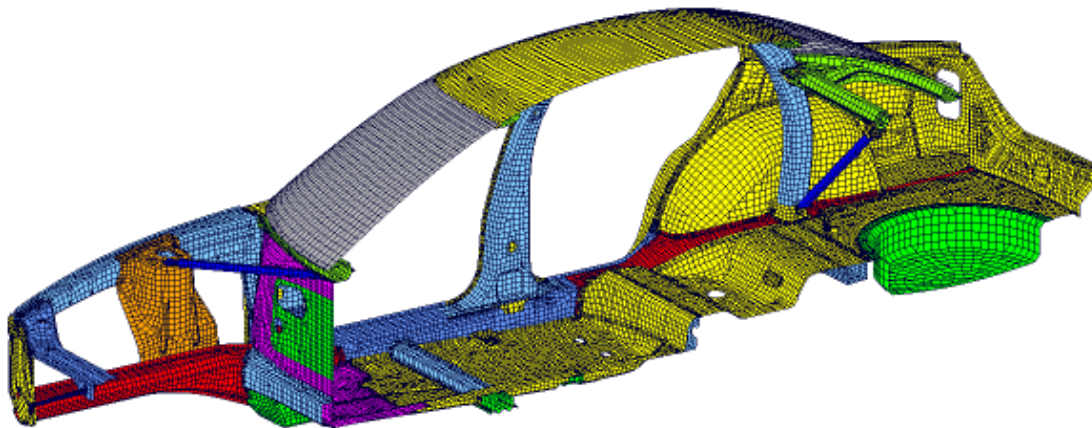


Figure 6.2-1 FE-Model

The stiffness model (per half model) consisted of:

- 54521 shell elements
- 53460 nodes

The deformed shapes for the load cases torsion and bending are shown in the Figures 6.2.1-1 and 6.2.2-1. To view the stiffness distribution vs. the x-axis, the diagrams 6.2.1-2 (torsion) and 6.2.1-3 (bending) are used. The derivation vs. the x-axis for torsion (Fig. 6.2.1-3) and bending (Fig.6.2.2-3) as well as the strain energy contour plots (Fig. 6.2.1-4 and Fig. 6.2.2-4) show the sensitive areas. The colored areas of the strain plots show the elastic energy, which is a result of the

deformation stored in the structure, as internal energy. The deformed shape of the dynamic stiffness simulation, the normal modes are shown in the Figures 6.2.3-1 to 6.2.3-3. The deformed frequency mode belongs to the normal modes mentioned in Table 6.2-2.

CAE Structural Performance	
Static Torsional Stiffness	21310 Nm/deg
Static Bending Stiffness	20540 N/mm
CAE Mass* (with glass)	230.6 kg
CAE Mass* (without glass)	202.8 kg
First Torsion Mode	61.4 Hz
First Bending Mode	61.8 Hz
Front End Lateral	60.3 Hz

*Mass as in test configuration (Chapter 6, page 2), brackets and reinforcements (6.4 kg) are not included (see Chapter 5, page 10)

Figure 6.2-2 Table of CAE Structural Performance

6.2.1. Torsional Stiffness

A load of 1000 N was applied at the shock tower front while the body structure was constrained at the rear center spring attachment in the lateral and vertical directions.

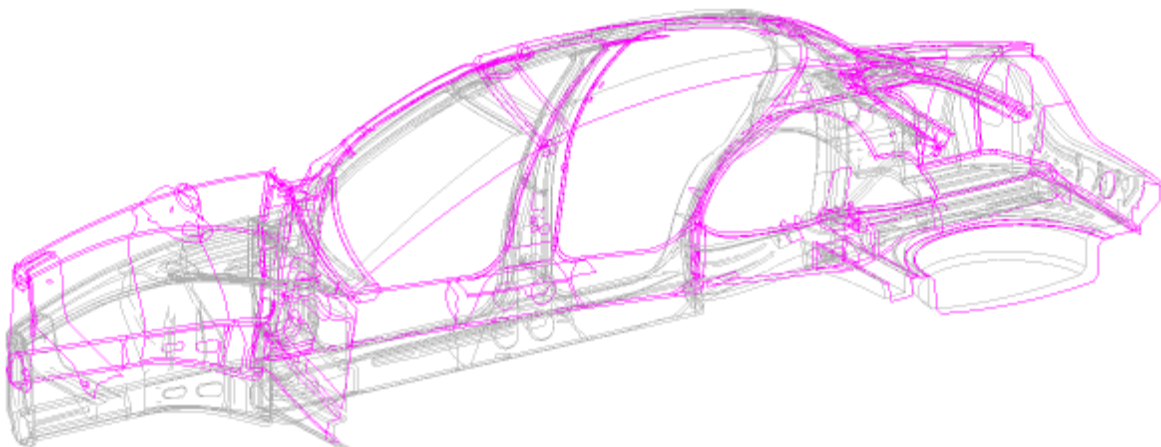


Figure 6.2.1-1 Deformed Shape for Torsion

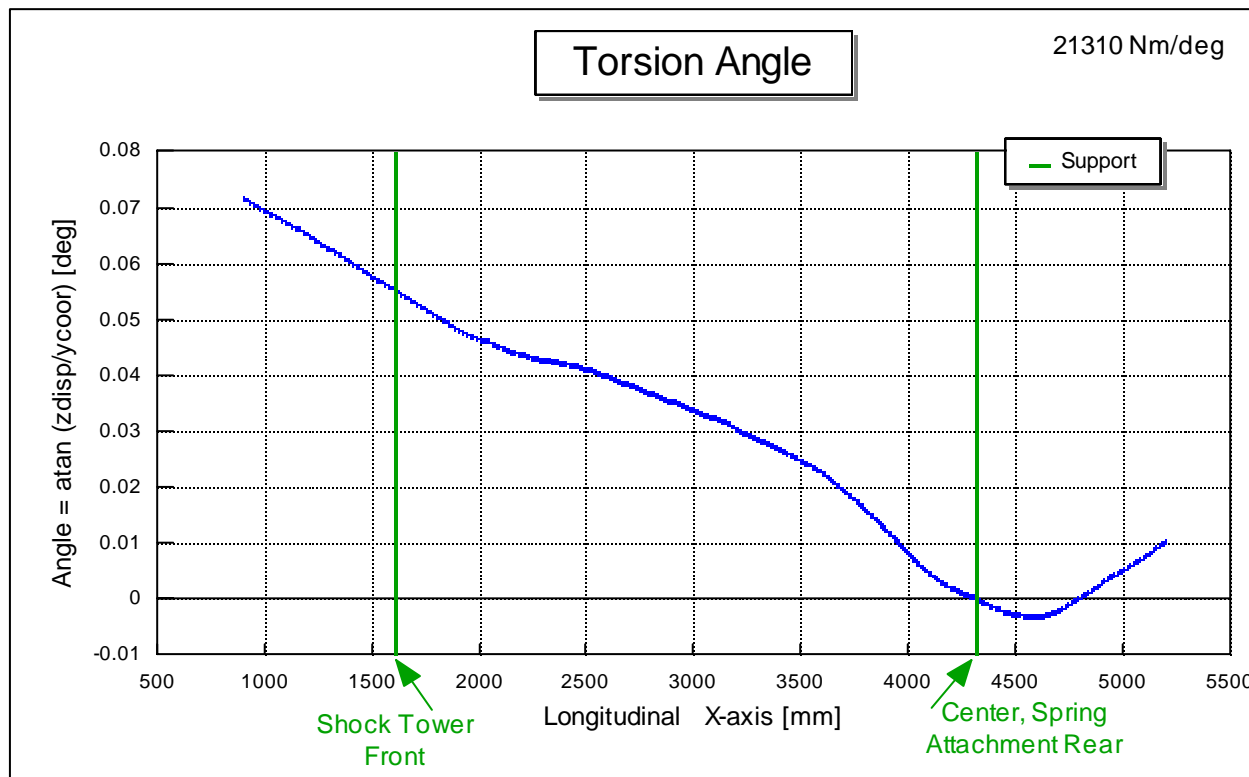


Figure 6.2.1-2 Torsion Angle vs. x-Axis

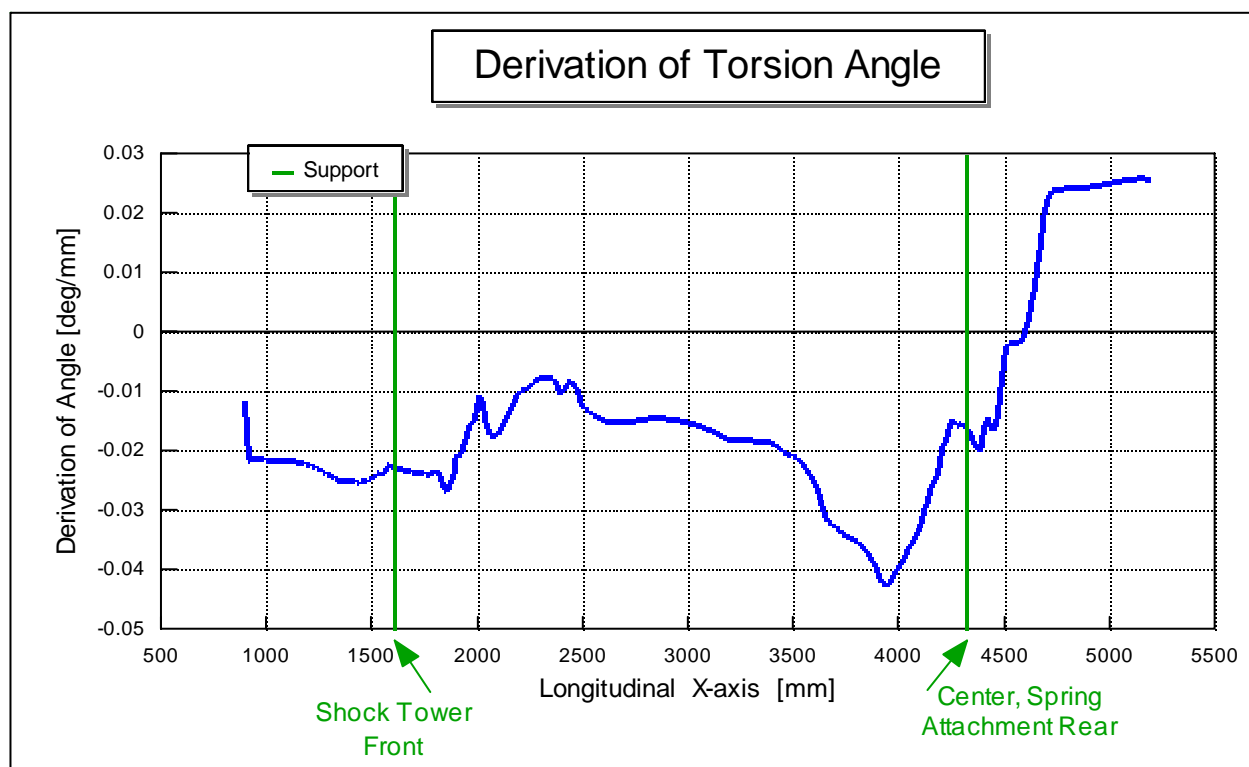


Figure 6.2.1-3 Derivation of Torsion Angle vs. x-Axis

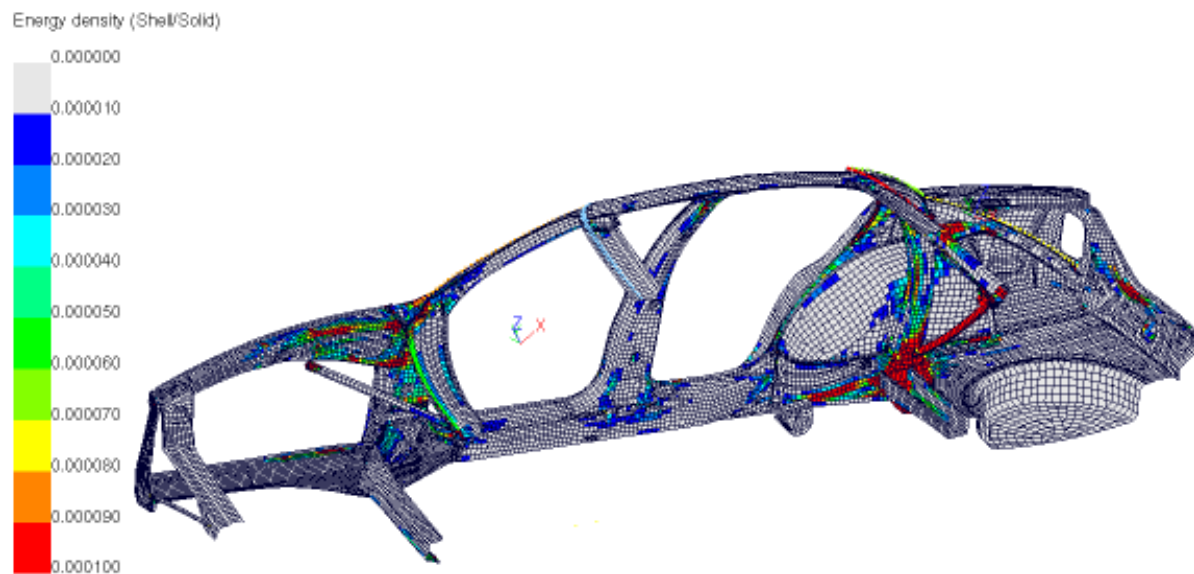


Figure 6.2.1-4 Strain Energy Contour Plot for Torsion

6.2.2. Bending Stiffness

The loads were applied to the center of the front seats and to the center of the two outer rear seats. The measurements were taken under a load of $F_{b \max} = 4000 \text{ N}$ ($4 \times 1000 \text{ N}$).

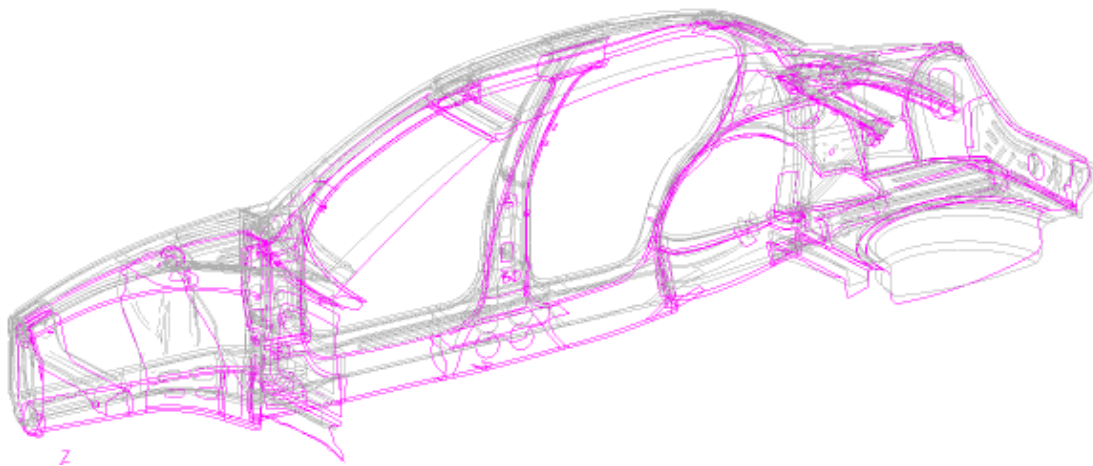


Figure 6.2.2-1 Deformed Shape for Bending

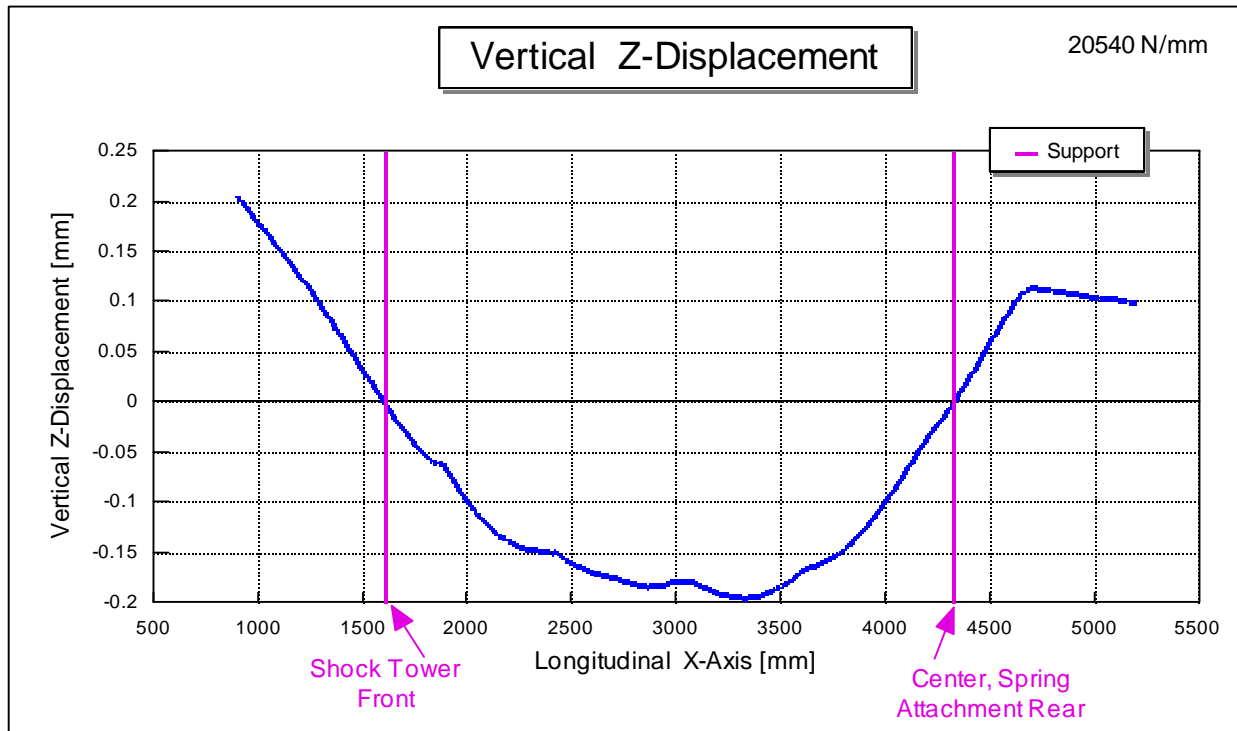


Figure 6.2.2-2 z-Displacement vs. x-Axis, Bending

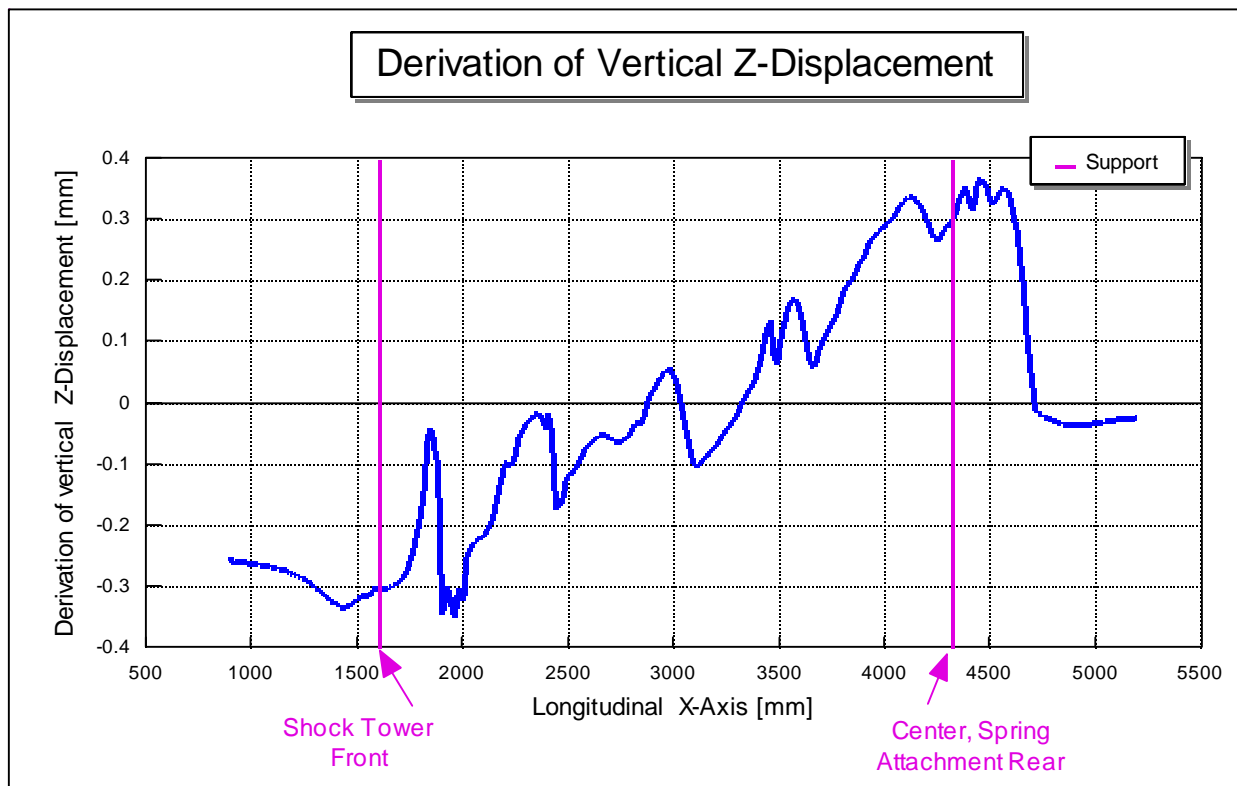


Figure 6.2.2-3 Derivation of z-Displacement vs. x-Axis, Bending

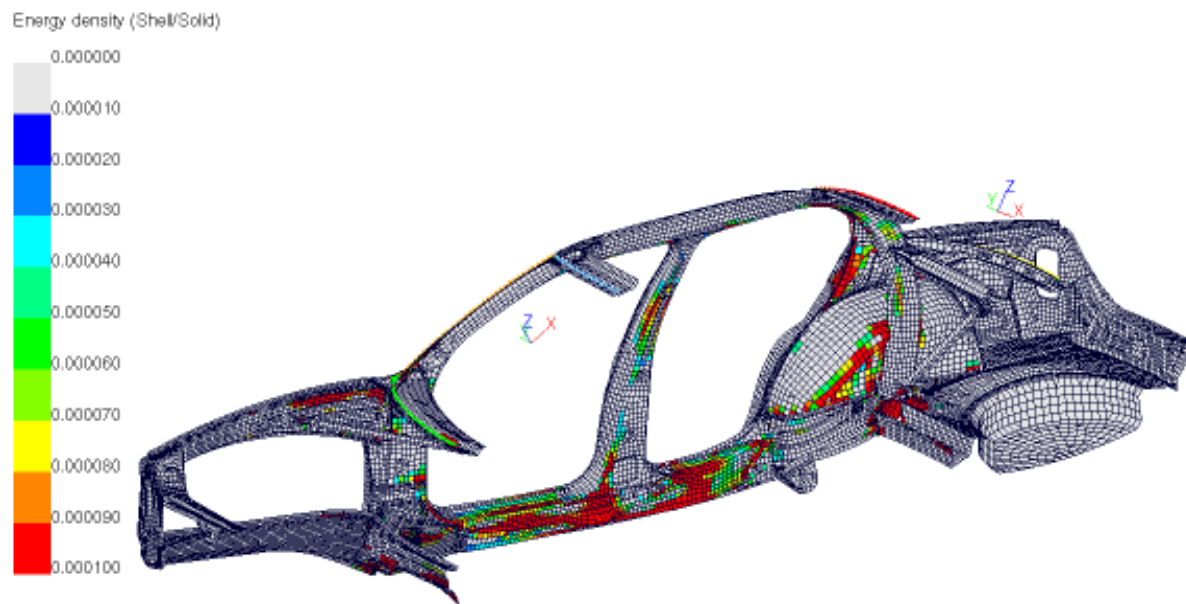


Figure 6.2.2-4 Strain Energy Contour Plot for Bending

6.2.3. Normal Modes

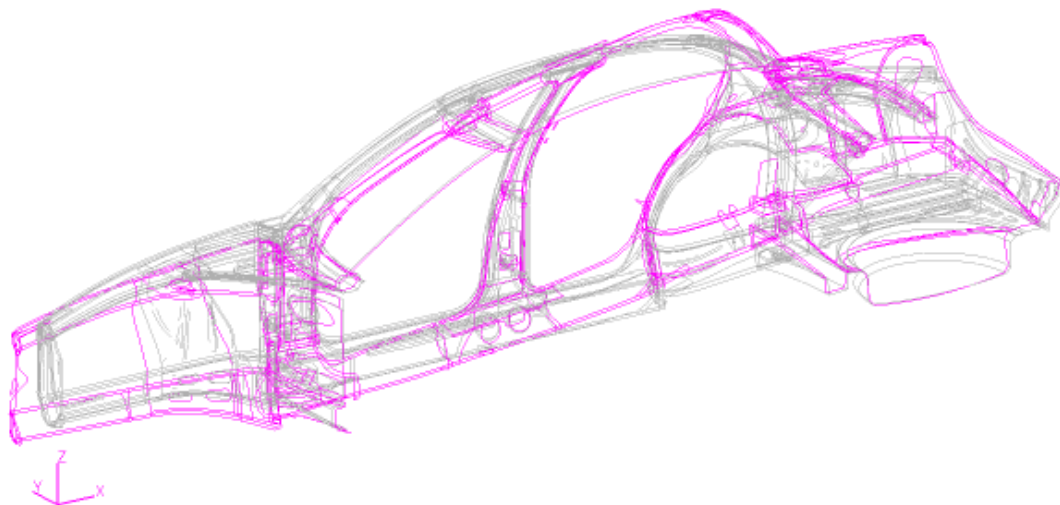


Figure 6.2.3-1 Front End Lateral Mode

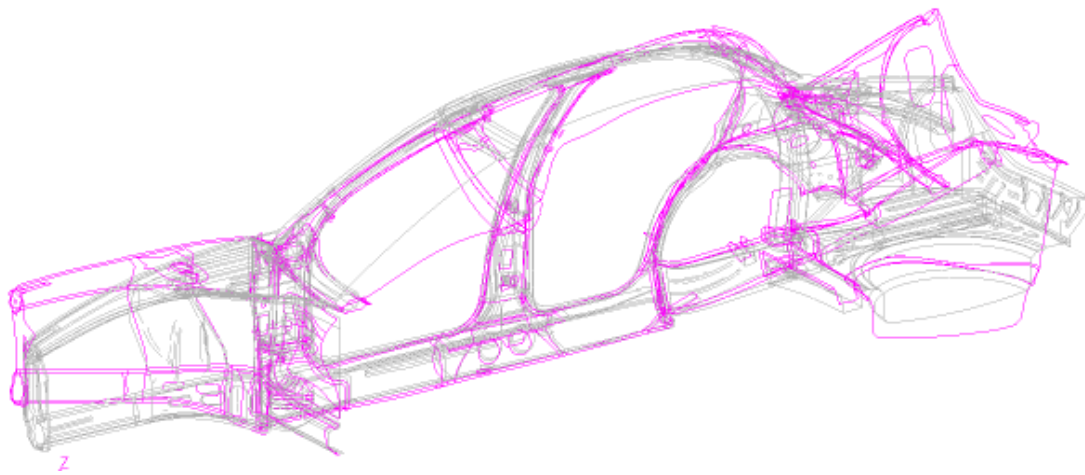


Figure 6.2.3-2 First Bending Mode

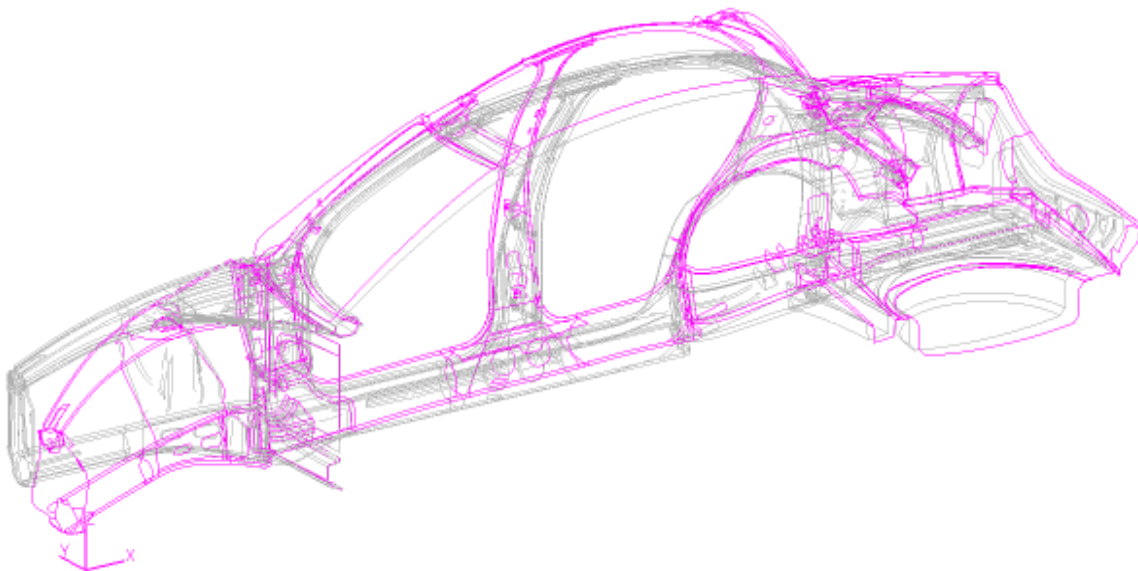


Figure 6.2.3-3 First Torsion Mode

6.3. Crash Analysis

For three crash types of the ULSAB project, one common crash model was generated. With this model the crash simulations were conducted:

- AMS 50% frontal offset crash at 55 km/h
- NCAP 100% frontal crash FMVSS 208 at 35 mph
- Side impact crash at 50 km/h (96/27 EG with deformable barrier)

For the rear crash (FMVSS 301) at 35mph only a half structure (Fig. 6.3.3-1) was used. Fig. 6.3-1 shows the high level of detail for the FE-Model. To realize a realistic crash behavior of the simulation, all the spot welds and laser welded areas were considered in the models. To analyze the crash behavior, all crash-relevant car components were modeled, such as:

- Wheels with tire model
- Engine and transmission
- Steering system
- Chassis system with subframe
- Fuel tank
- Bumper system including crashbox
- Radiator with fan
- Battery
- Spare tire
- Brake booster, ABS box and cylinder
- Doors, front and rear without glass

The door concept used for all simulations was a typical two shell structure with an inner and outer panel, an upper door reinforcement and two high strength side impact beams at the front door and one side impact beam at the rear door.

A three point fixture with reinforcements at the hinges and the locks supported the doors.

To reduce the model size for the roof crush analysis, the full model with reduced contents was used (Fig. 6.3.5-1).

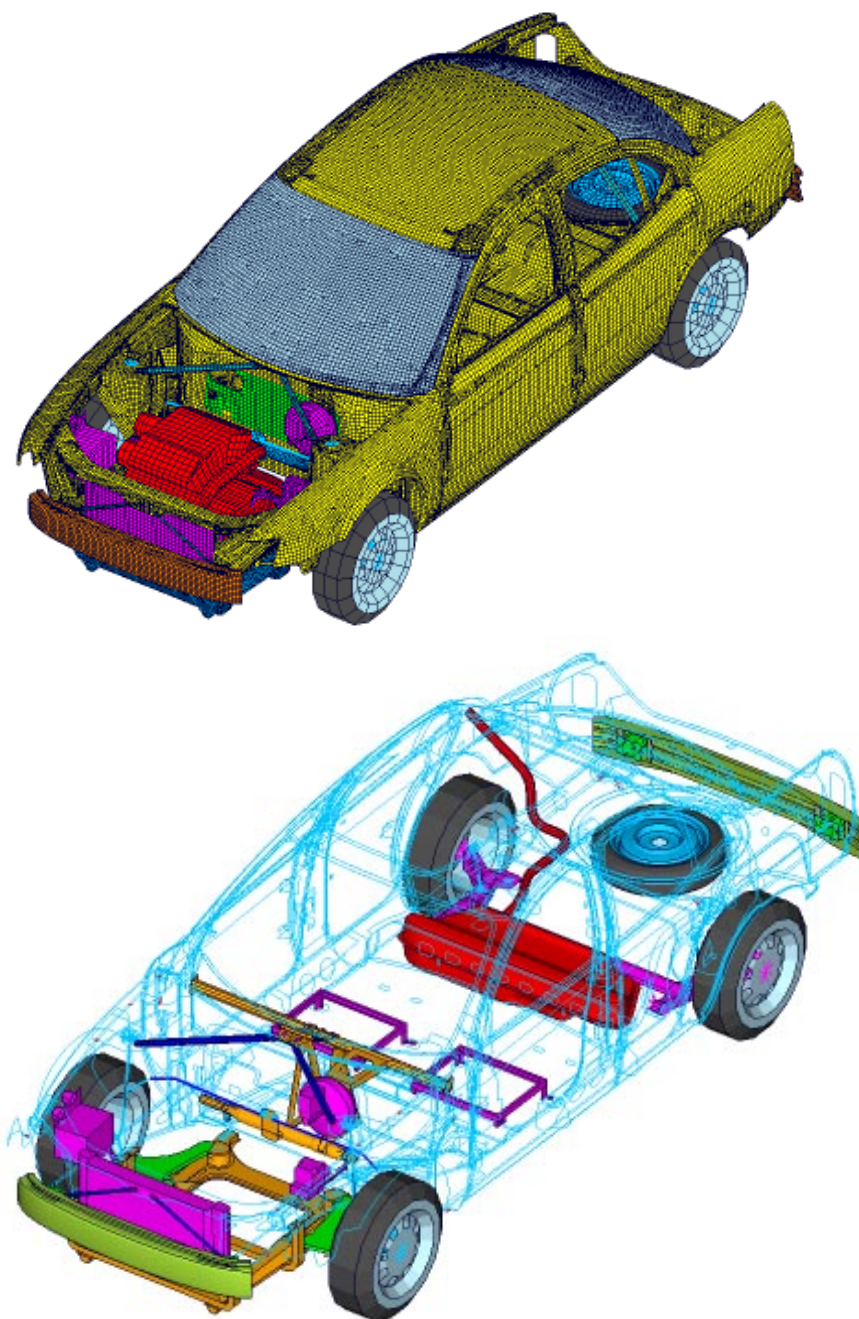


Figure 6.3-1 Crash Analysis Model

A high level of detail of the surfaces, welding and mounting locations was necessary to provide the resolution to be able to access the events. The LS-DYNA complete full model had 178386 elements and 174532 nodes.

The vehicle mass was defined to be base curb weight plus two 50th percentile male dummies with 113 kg of luggage. The crash mass of the vehicle was set at 1612 kg. The crash mass of the vehicle is calculated as follows:

Curb Mass	1350 kg
Luggage	113 kg
Dummies	149 kg
Total Crash Mass	1612 kg

6.3.1. AMS Offset Crash

The AMS offset crash was defined in the year 1990 by the editor of the German automotive magazine 'Auto Motor Sport' (AMS). The aim of this offset crash is to secure the passenger compartment residual space. For this requirement a stiff passenger compartment and a good energy absorption in the front structure is needed. The initial velocity for the car is 55 km/h for the AMS crash.

The Offset barrier is a block with a 15 degree rotated contact area including two anti-slide devices mounted on the contact surface. The left side of the car hits the barrier with an overlap of 50%.

For actual crash tests AMS analyzes the following values:

- HIC-value (Head Injury Criterion)
- Head, chest and pelvis acceleration
- Maximum belt forces
- Maximum femur forces
- Dynamic steering deformation
- Foot well intrusions
- Door opening after test

Because the analysis did not include dummies, injury assessment could not be made. Injury performance is greatly affected by the structural crash and steering column movement as well as by the knee bar design. Evaluation of passenger compartment intrusion can be made by looking at deformation in the foot well area (Fig. 6.3.1-4). Looking at the overall shape of the deformation (Fig. 6.3.1-2, -3 can assess structural integrity).

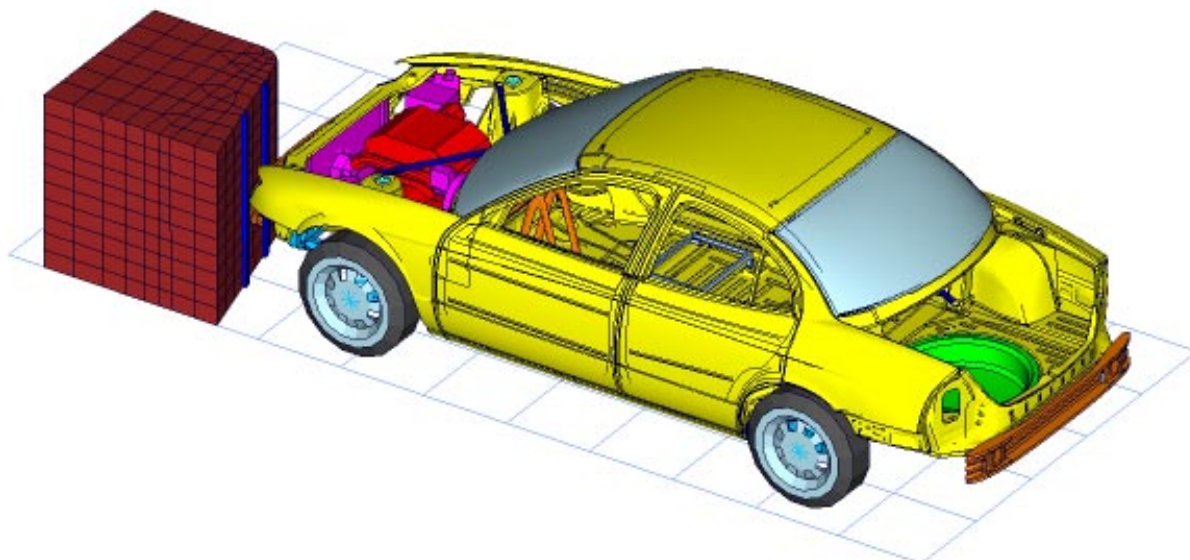
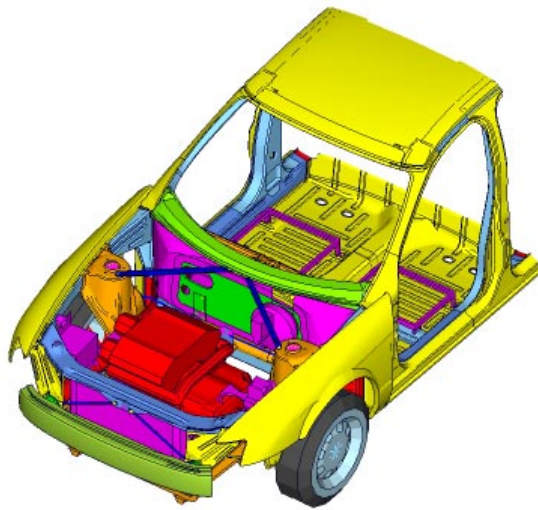


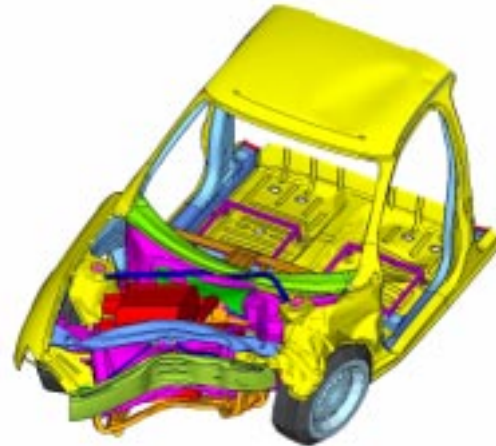
Figure 6.3.1-1 AMS Offset Crash Analysis Setup

The AMS Offset undeformed and deformed shapes are shown in Fig. 6.3.1-2 and 6.3.1-3. The deformed shape in these figures is after 100 ms. The deformation in the footwell area is shown in Fig. 6.3.1-4. The analyzed deformation is measured in the foot well area where it is important to keep the deformations as low as possible, because of the injury of the passenger's legs.

The internal energy absorption diagram in Fig. 6.3.1-5 gives an overview of the internal energy absorbed in the parts subframe, bumper beam, crashbox, front rail and fender side rail after 100 ms. The diagram in Fig. 6.3.1-6 shows the load path for the most important front structure components. The diagram shows the main load path is the rail front. The fender side rail and the subframe have about the same load level. The diagram, AMS Offset Crash Acceleration vs. Time (Fig. 6.3.1-7) shows an average acceleration calculated from the rocker LHS, tunnel, and rocker RHS. After the contact between AMS barrier and engine, a middle acceleration of about 25 g results in the passenger area. The Figure 6.3.1-8 shows the function of the car deformation versus time. After about 90 ms the maximum dynamic deformation is reached.

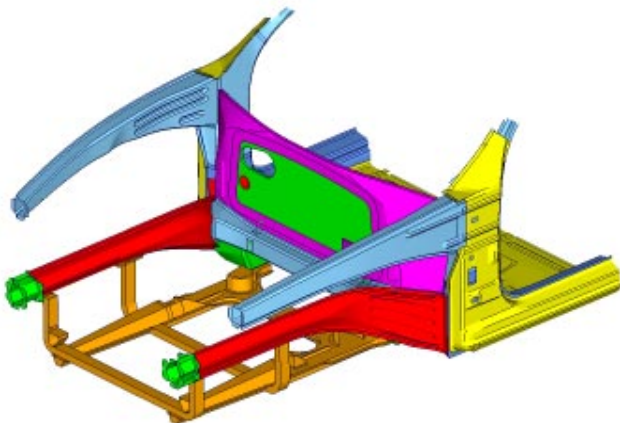


$t = 0 \text{ ms}$

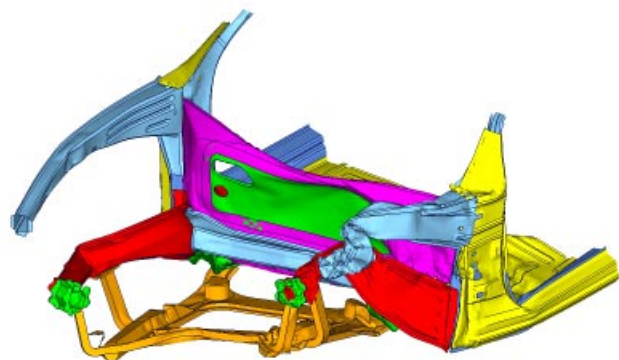


$t = 100 \text{ ms}$

Figure 6.3.1-2 AMS Offset Crash Deformed Shapes



$t = 0 \text{ ms}$



$t = 100 \text{ ms}$

Figure 6.3.1-3 AMS Offset Crash Deformed Shapes of Longitudinals

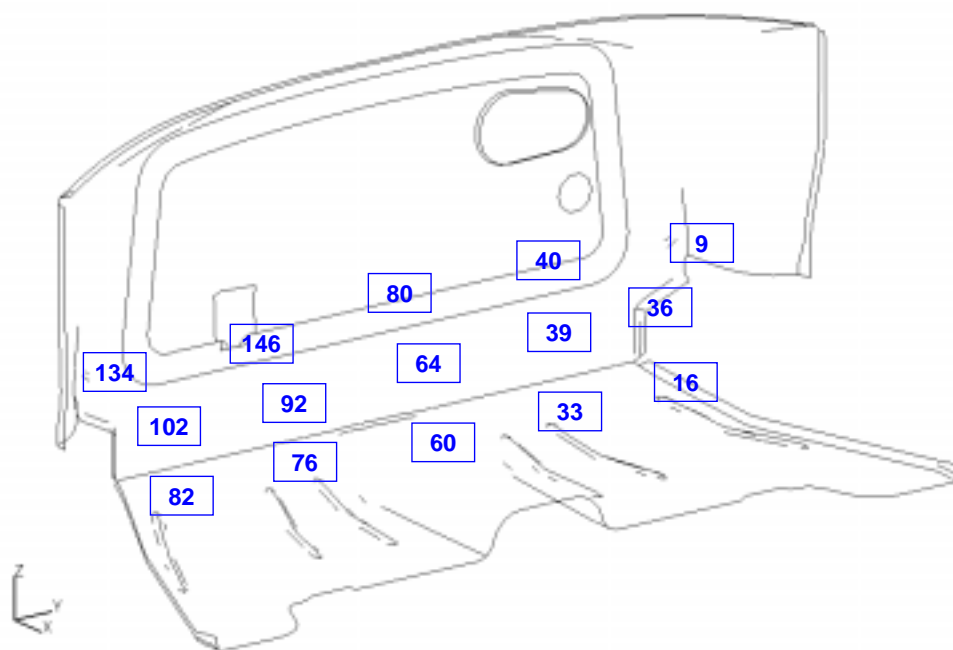


Figure 6.3.1-4 AMS Offset Crash Maximum Dynamic Foot Room Intrusion in mm

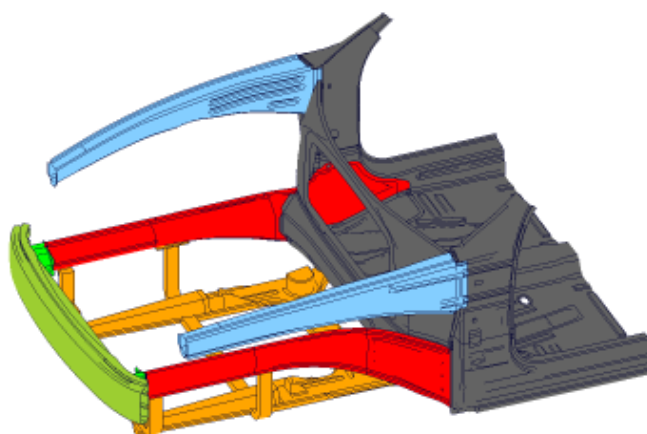
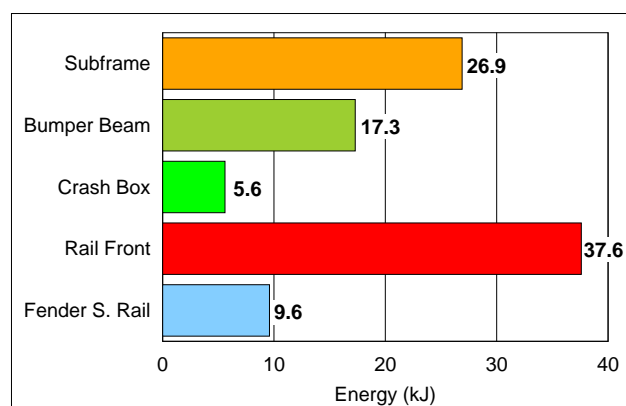


Figure 6.3.1-5 AMS Offset Crash Internal Energy Absorption

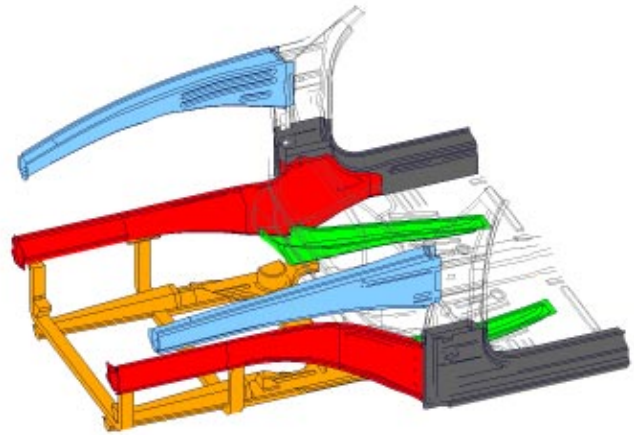
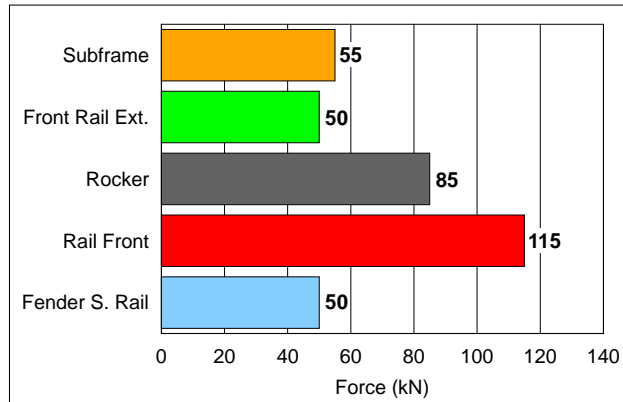


Figure 6.3.1-6 AMS Offset Crash Typical Cross Section Forces

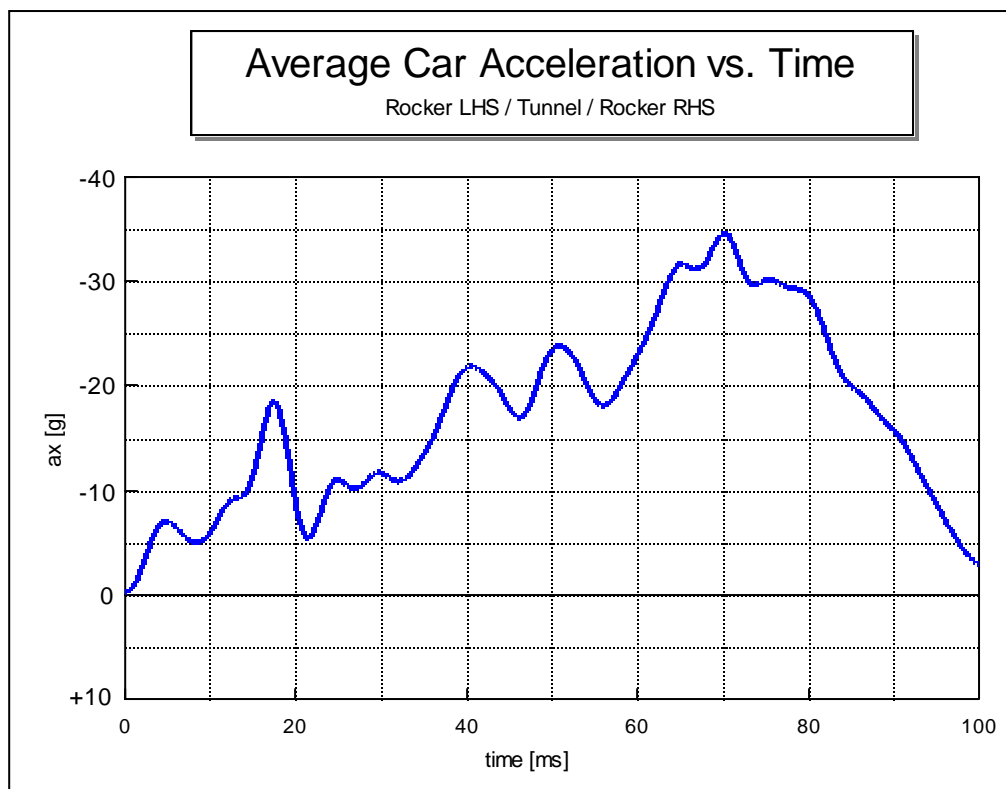


Figure 6.3.1-7 AMS Offset Crash Acceleration vs. Time

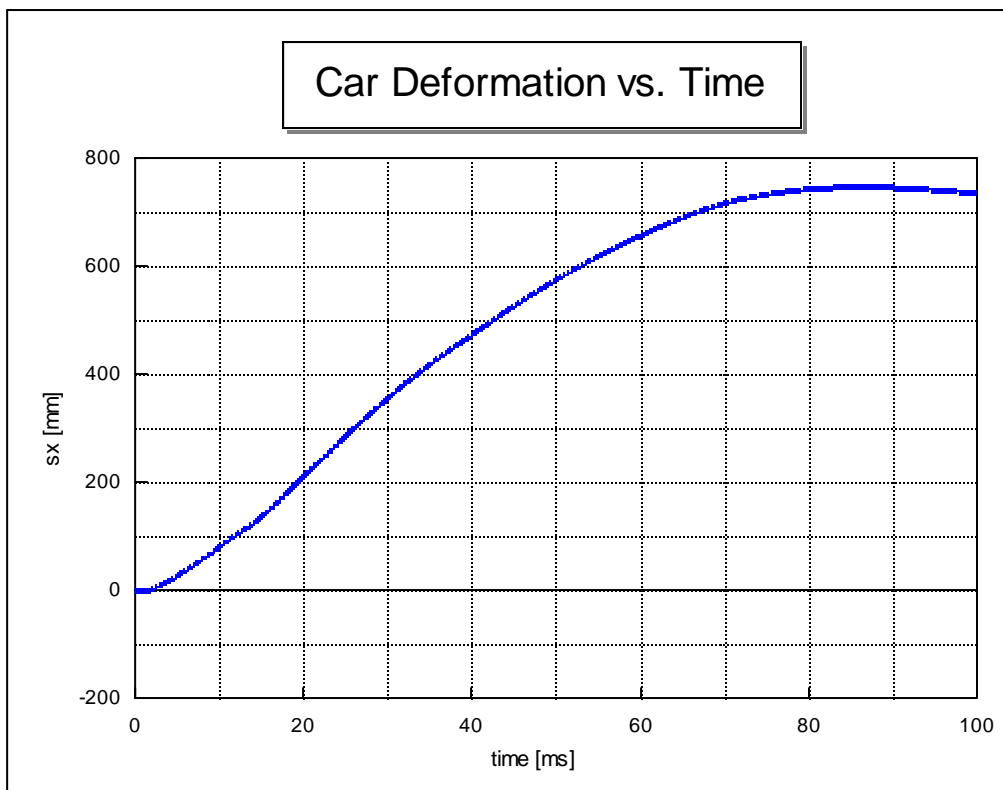


Figure 6.3.1-8 AMS Offset Crash Deformation vs. Time

In the following table (Fig. 6.3.1-9), the AMS crash events vs. time are explained:

Time (ms) AMS Offset Crash	
12.00	Initial folding of longitudinal LHS
16.00	Initial folding of subframe
18.00	First buckling of rail upper in front of shock tower
36.00	Wheel LHS contacts barrier
40.00	Engine contacts barrier, start of vehicle-rotation around z-axis
44.00	Deformable front end of the subframe totally deformed, stiffer rear end and the extension longitudinal LHS starts moving rearwards and causes deformation in the front floor area, buckling of the longitudinal in the area of the shock tower
48.00	Second buckling of rail upper LHS behind the shock tower
52.00	Buckling of the rear end of the subframe at the fixture on the extension longitudinals
60.00	Buckling of the brace cowl to shock tower LHS. Engine hits the steering gear.
68.00	Contact between gearbox-mounting and brake booster
70.00	Wheel LHS hits the hinge pillar
88.00	Maximum dynamic deformation reached

Figure 6.3.1-9 AMS Offset Crash Events

This analysis shows good progressive crush on the barrier side (left), as well as crush on the right, indicating transfer of load to the right side of the structure. This transfer means that the barrier side is not relied upon solely to manage the crash event.

This transfer also contributes to the preservation of the occupant compartment. The intrusion of 146 mm into the footwell is minimal given the severity of this event.

The initial, early peak shown in the pulse graph should trigger air bag systems.

Peak deceleration of approximately 35 gs, a good result considering the severity of this event.

6.3.2. NCAP 100% Frontal Crash

The conditions for the front crash analysis are based on several requirements. In the ULSAB program, the focus was on progressive crush of the upper and lower load path, sequential stack up of the bumper, radiator, and powertrain, integrity between individual components, A-pillar displacement, definition of the door opening, uniform distribution of the load, toe pan intrusion, and passenger compartment residual space. These requirements contribute towards occupant safety and the United State Federal Motor Vehicle Safety Standard, FMVSS 208.

The test sequence of the front crash analysis is set up to duplicate a 35 mph, National Highway and Traffic Safety Association (NHTSA) full frontal barrier test (Fig. 6.3.2-1).

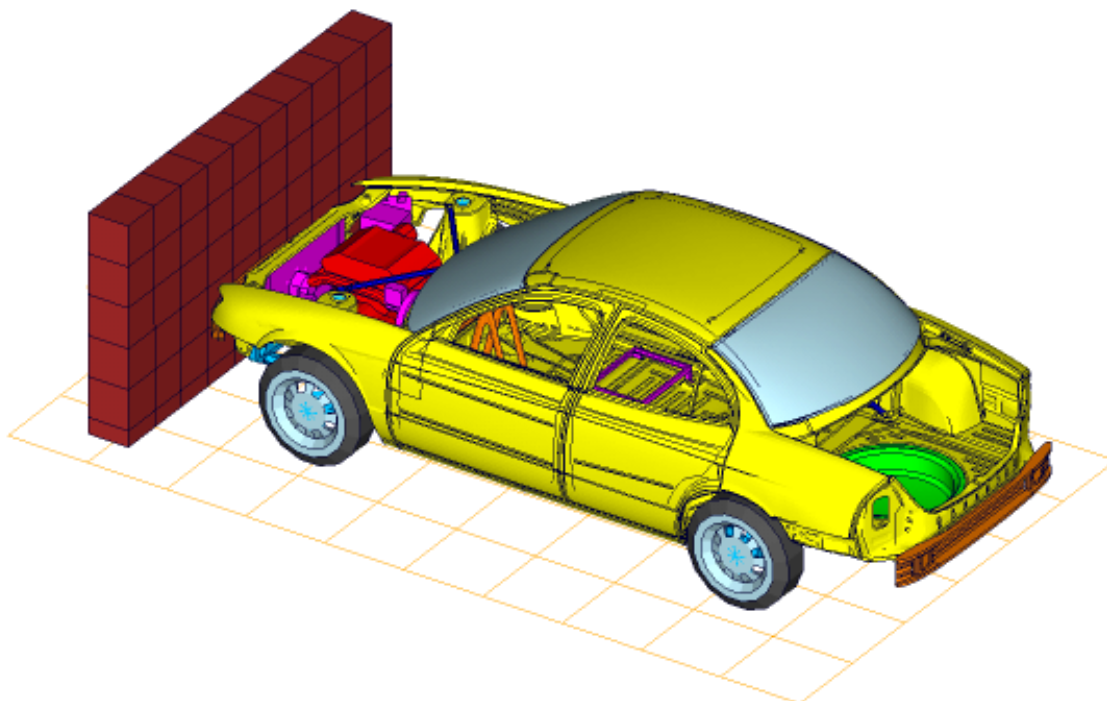


Figure 6.3.2-1 NCAP 100% Crash Analysis Setup

The NCAP 100% Frontal Crash undeformed and deformed shape is shown in Figures 6.3.2-2 and 6.3.2-3. The deformed shape in the figure is after 100 ms. The deformation in the footwell area is shown in Fig. 6.3.2-4. The analyzed deformations are measured in the foot well area where it is important to keep the deformations as low as possible, because of the injury of the passenger legs.

The internal energy absorption diagram in Fig. 6.3.2-5 gives an overview of the internal energy absorbed in the parts subframe, bumper beam, crashbox, front rail and fender side rail after 100 ms. The diagram in Fig. 6.3.2-6 shows the section force for the most important front structure components. The diagram shows that the main load path is the rail front. The components, fender side rail and the subframe have about the same load level. The diagram, NCAP Crash Acceleration vs. Time (Fig. 6.3.2-7), is an average of accelerations at the rocker LHS, tunnel, and rocker RHS. After the contact between barrier and engine it results a middle acceleration of about 29 g at the passenger area. The Figure 6.3.2-8 shows the function of the car deformation versus time. After about 68 ms the maximum dynamic deformation is reached.

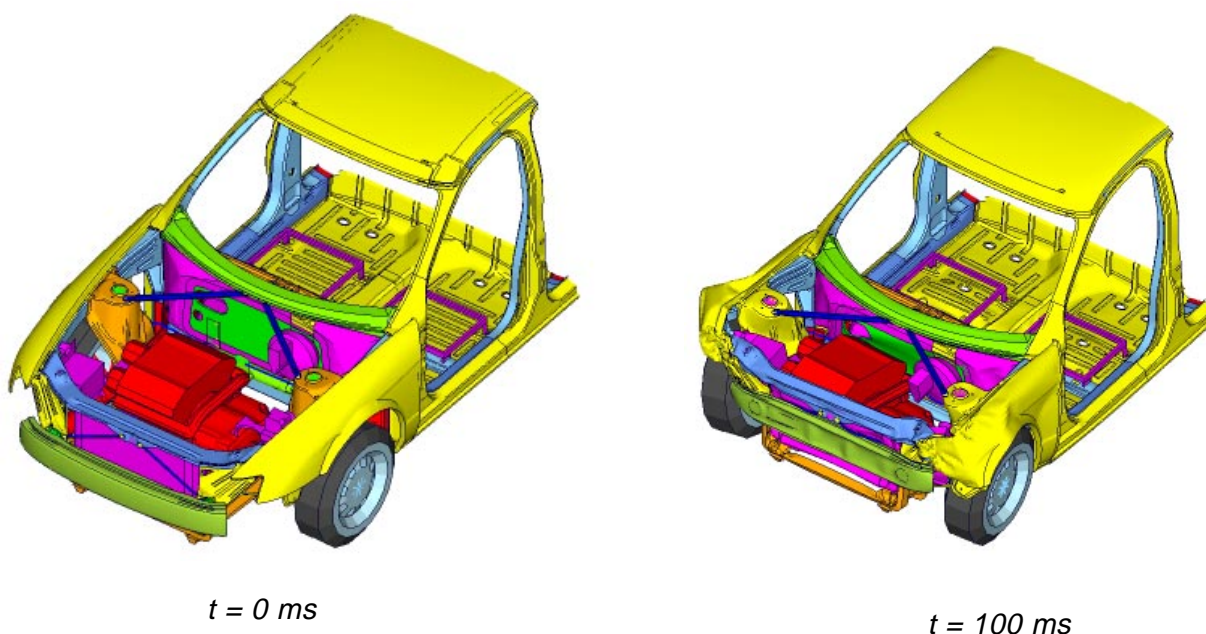


Figure 6.3.2-2 NCAP 100% Crash Deformed Shapes

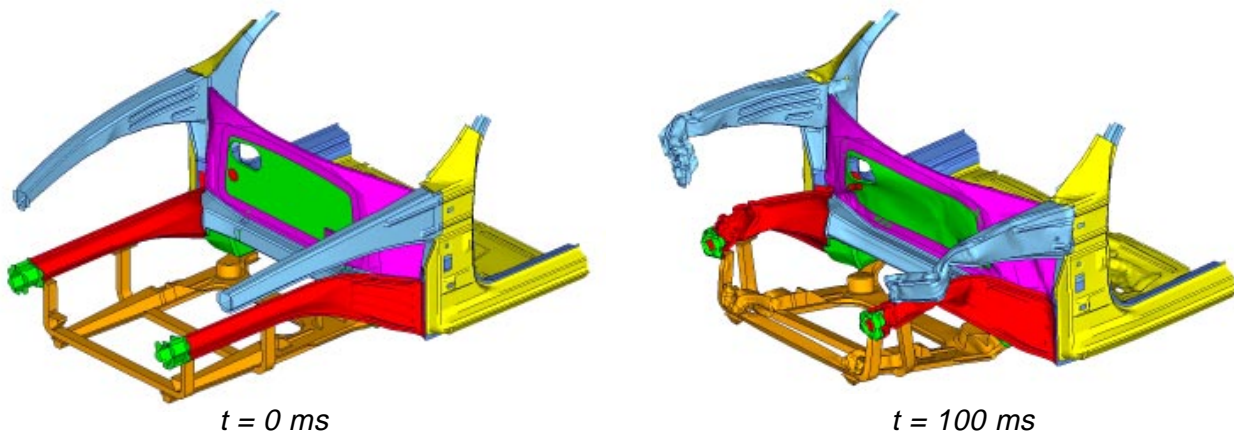


Figure 6.3.2-3 NCAP 100% Crash Deformed Shapes of Longitudinals

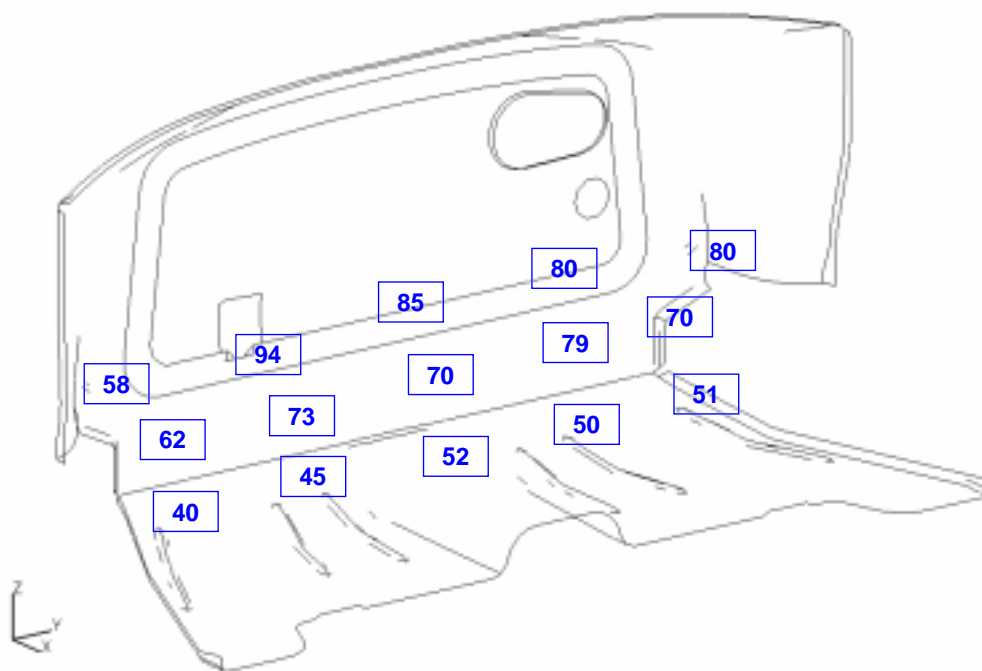


Figure 6.3.2-4 NCAP 100% Crash Maximum Dynamic Foot Room Intrusion in mm

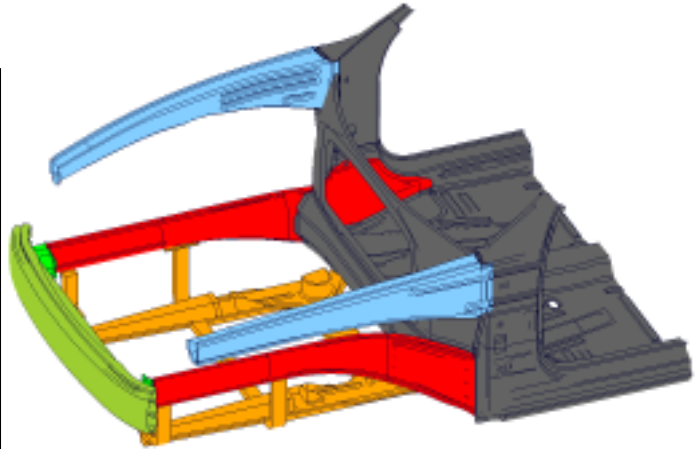
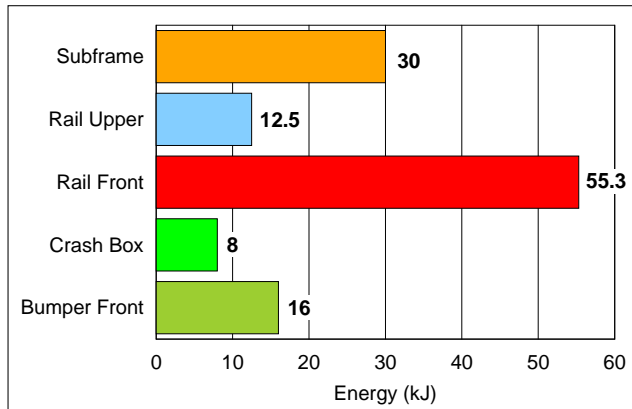


Figure 6.3.2-5 NCAP 100% Crash Internal Energy Absorption

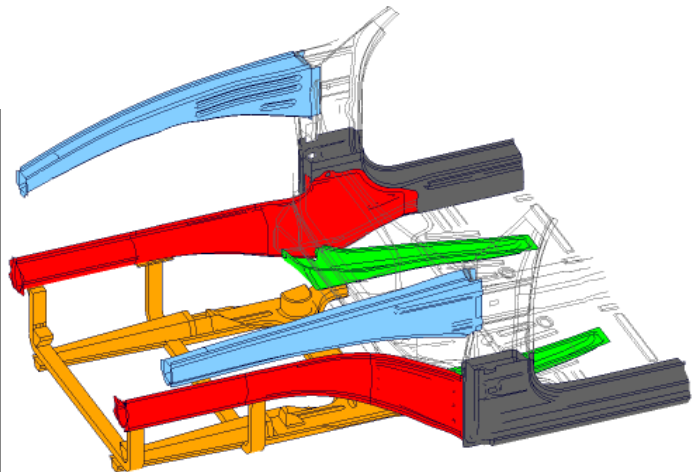
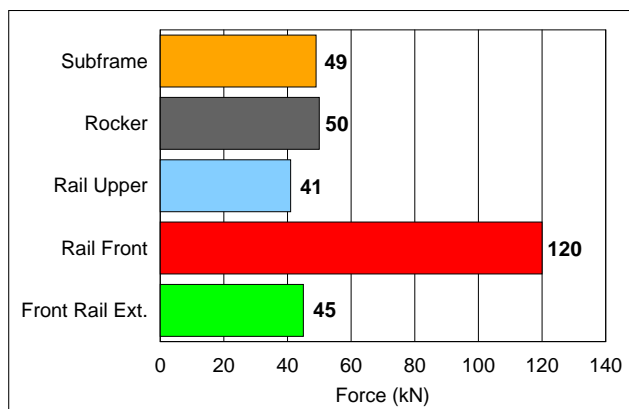


Figure 6.3.2-6 NCAP 100% Crash Typical Cross Section Forces

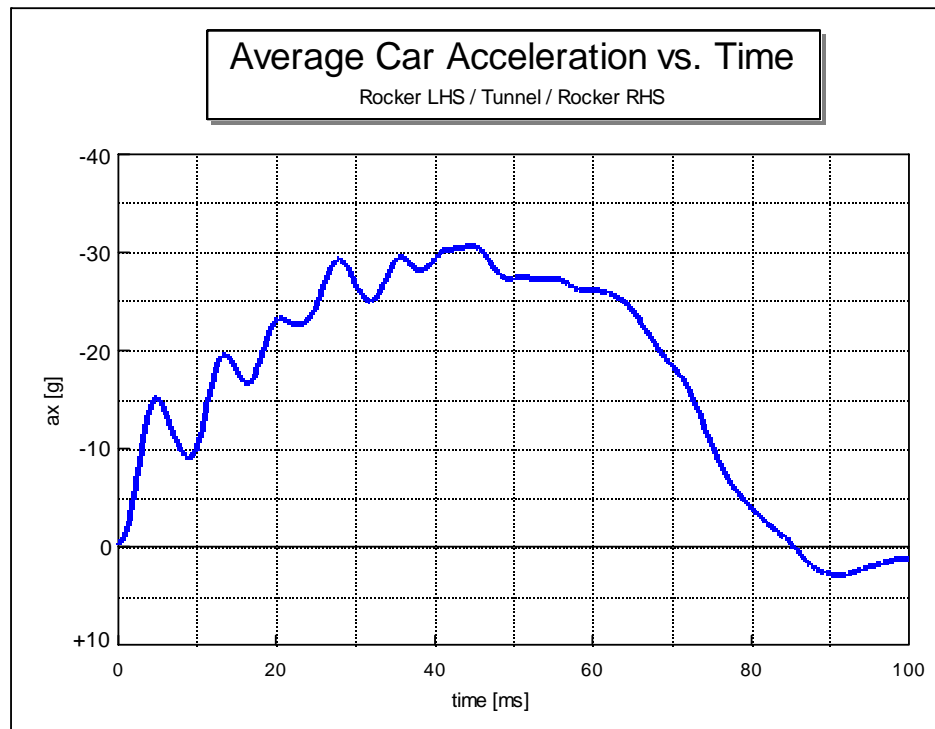


Figure 6.3.2-7 NCAP 100% Crash Acceleration vs. Time

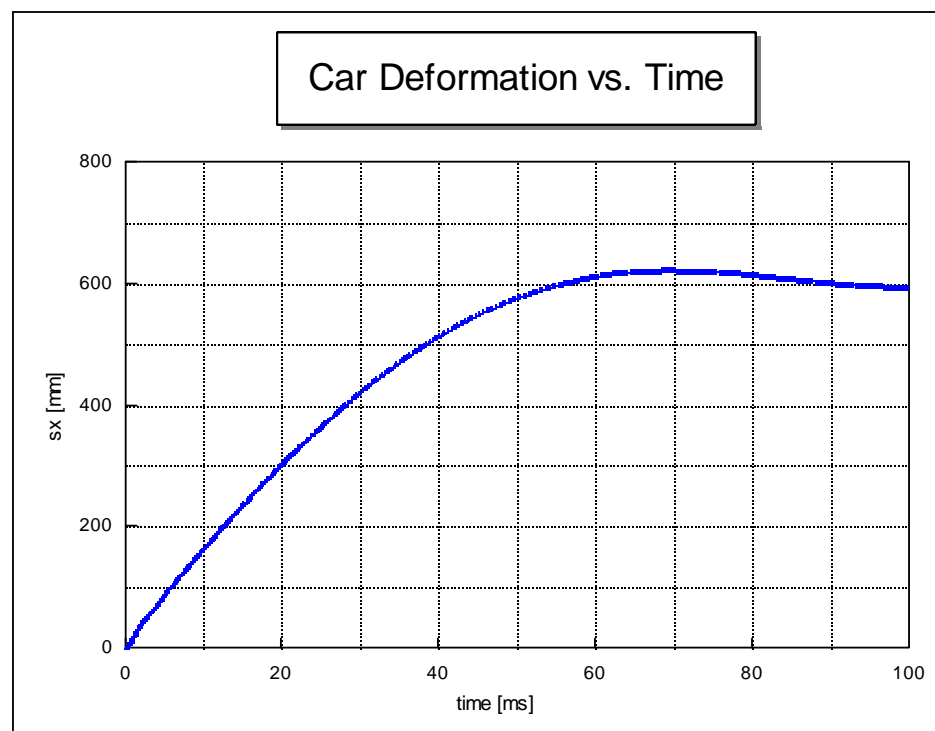


Figure 6.3.2-8 NCAP 100% Crash Deformation vs. Time

The following table (Figure 6.3.2-9) shows the NCAP crash events:

Time (ms)	NCAP Front Crash
12.00	Initial folding of longitudinal
16.00	Initial folding of subframe
21.00	First buckling of rails upper in front of shock tower
35.00	Engine contacts barrier
37.00	Buckling of the rear end of the subframe at the fixture on the extension longitudinals
50.00	Rear end of longitudinals start to buckle behind the reinforcement (still stable)
51.00	Wheels contacts barrier
67.00	Maximum dynamic deformation reached

Figure 6.3.2-9 NCAP Front Crash Events

This analysis illustrates good progressive crush of the upper and lower structure and subframe. It shows peak deceleration of 31 gs, which is satisfactory considering that this structure is designed with stiffer body sides to meet 50% AMS offset crash requirements.

The pulse graph is sympathetic to current occupant restraint systems. It shows a consistent rise to the peak of 31 gs then a smooth ride down to zero, indicating that the occupant would experience controlled restraint. The initial, early peak should trigger air bag systems. Low intrusion at the footwell indicates that leg damage is unlikely.

6.3.3. Rear Crash

The conditions for the rear impact analysis are based on the United States Rear Moving Barrier Test FMVSS-301. The test specifically addresses fuel system integrity during a rear impact. Automotive companies also include structural integrity and passenger compartment volume as additional goals for this test.

The impacting barrier is designed to represent a worst case rear crash (Fig. 6.3.3-1). The rear crash barrier is a rigid body with a mass of 1830 kg, making contact at zero degrees relative to the stationary vehicle. The Federal Standard identifies that the velocity of the rear moving barrier is 30 mph. The ULSAB program has raised the standard to 35 mph, which is 36% more kinetic energy of the moving barrier.

Evaluating fuel system integrity is done by representing a fuel tank system. The additional goals of passenger compartment integrity, residual volume, and door opening after the test can be addressed by looking at the deformed shapes of the vehicle during the crash event. During the early stages of the impact, there should be a little or no deformation in the interior. This sequence of events (Fig. 6.3.3-8) is necessary up to the time that the tires make contact with the barrier face and transfer load to the suspension and the rear of the rocker panel.

For the rear crash a half structure model was used. The rear crash deformed shapes are shown in Fig 6.3.3-2. To analyze the rear passenger compartment integrity, Figure 6.3.3-3 shows that maximum dynamic intrusion in this area.

The diagram (Fig. 6.3.3-4) shows the energy absorption, and the cross sections of the main hood load paths are shown in Figure 6.3.3-5. Due to the results, the rear rail and the rocker were the most important hood paths of the rear structure.

The Rear Crash Acceleration vs. Time (Fig. 6.3.3-6) shows an average acceleration of the rocker RHS and the tunnel. Figure 6.3.3-7 shows the total car deformation, at approximately 85 ms, the maximum dynamic deformation was reached.

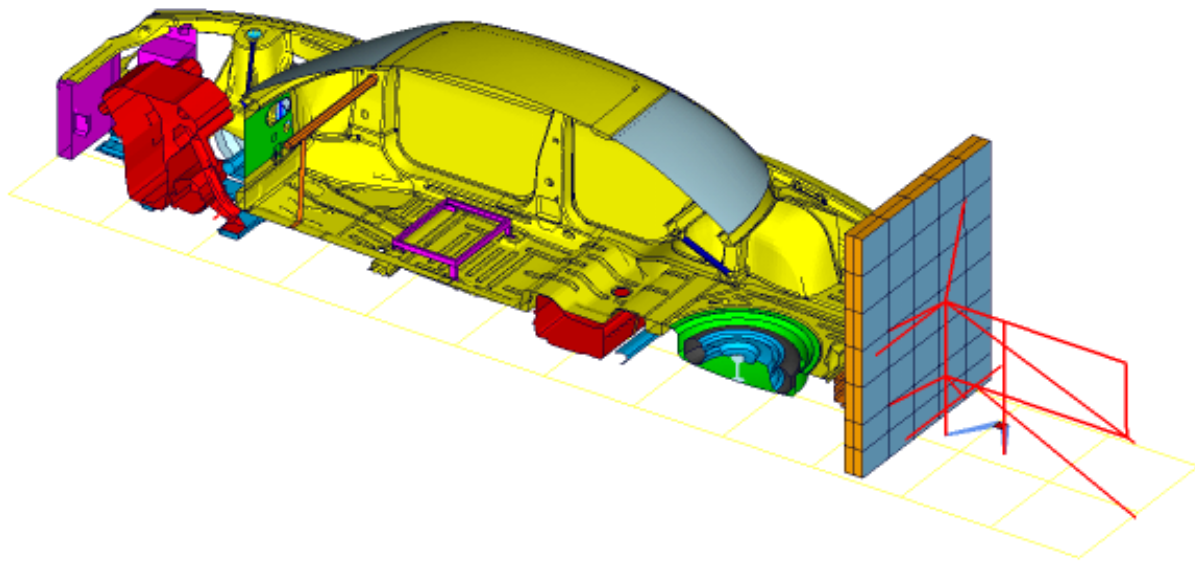
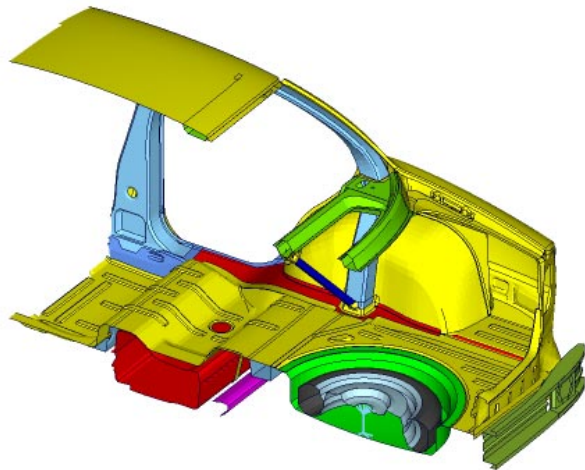
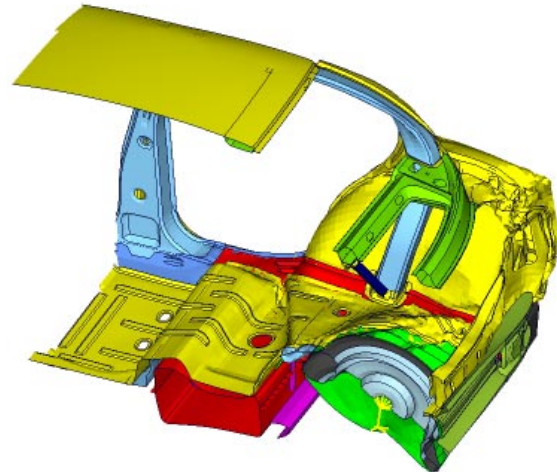


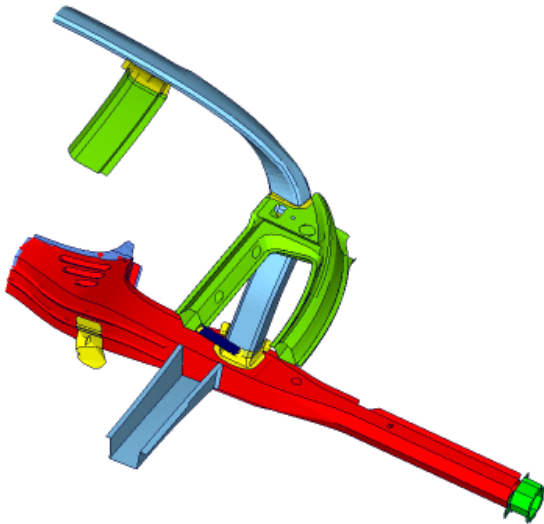
Figure 6.3.3-1 Rear Crash Analysis Setup



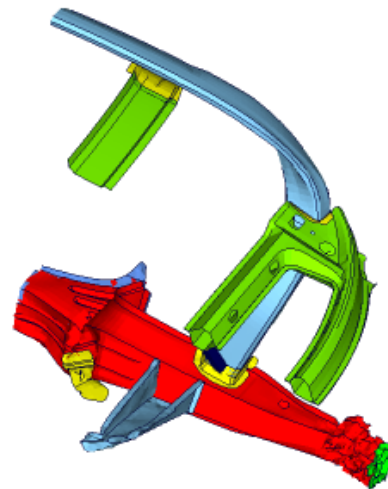
$t = 0$ ms



$t = 100$ ms



$t = 0$ ms



$t = 100$ ms

Figure 6.3.3-2 Rear Crash Deformed Shapes

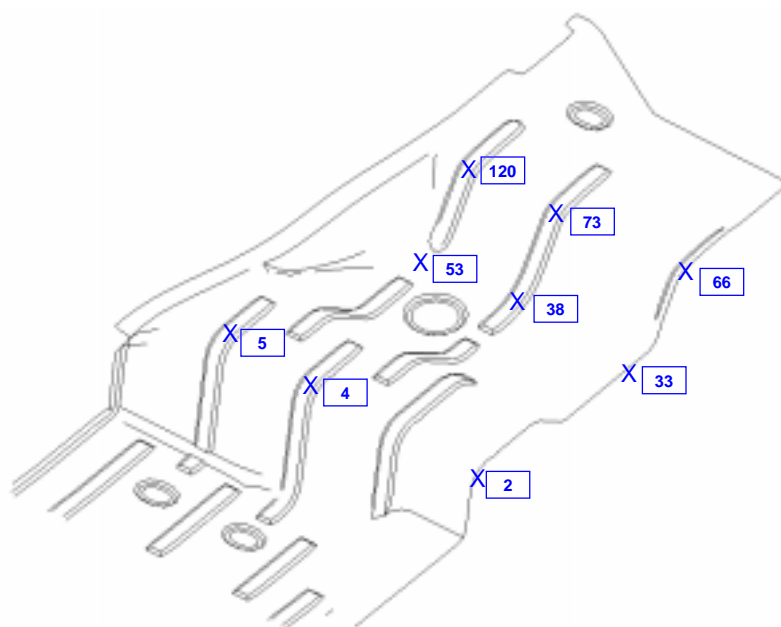


Figure 6.3.3-3 Rear Crash Maximum Dynamic Room Intrusion (mm)

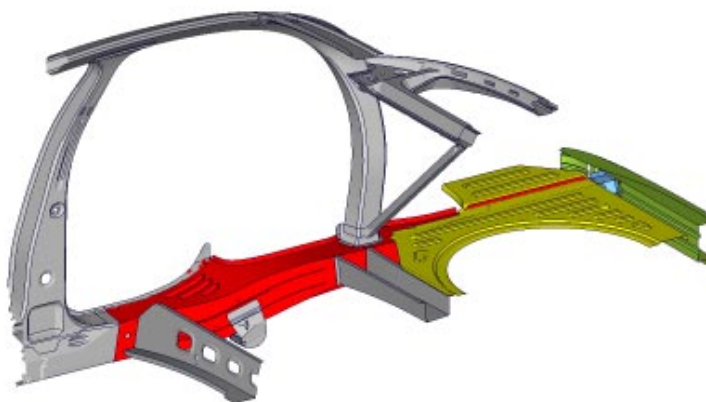
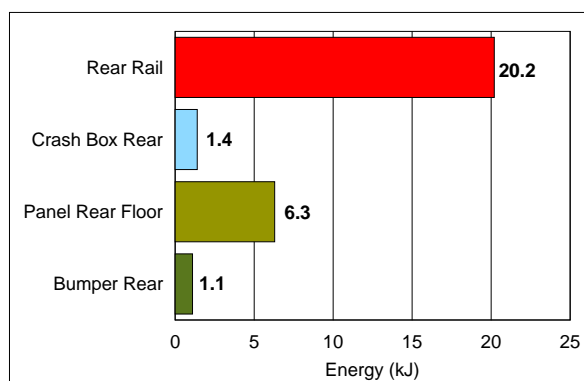


Figure 6.3.3-4 Rear Crash Internal Energy Absorption (kJ)

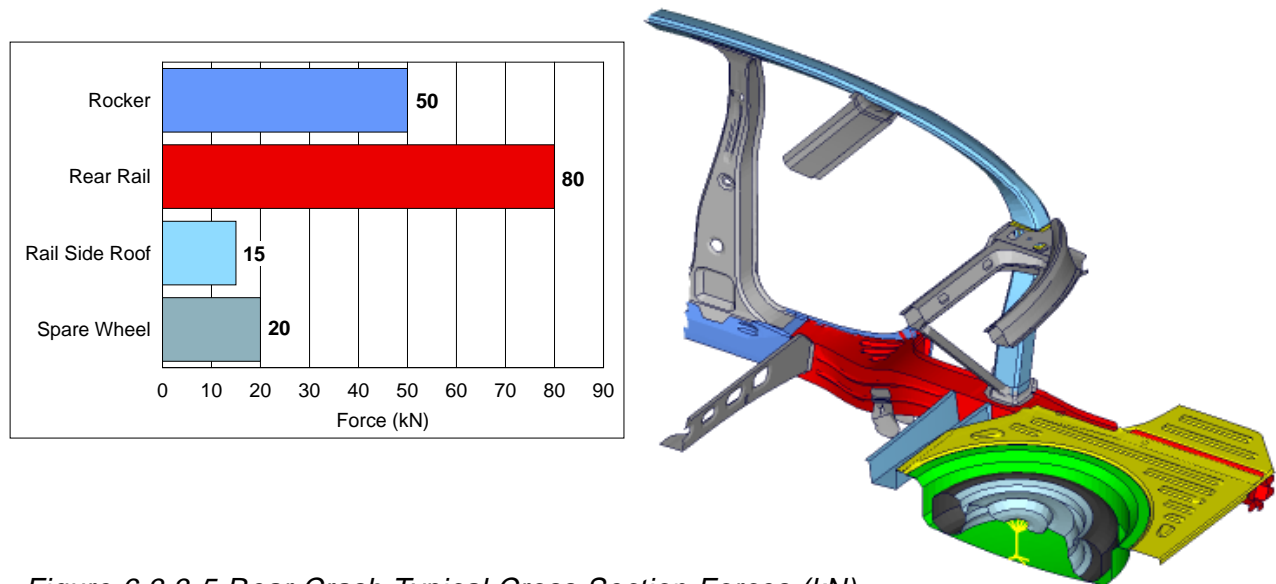


Figure 6.3.3-5 Rear Crash Typical Cross Section Forces (kN)

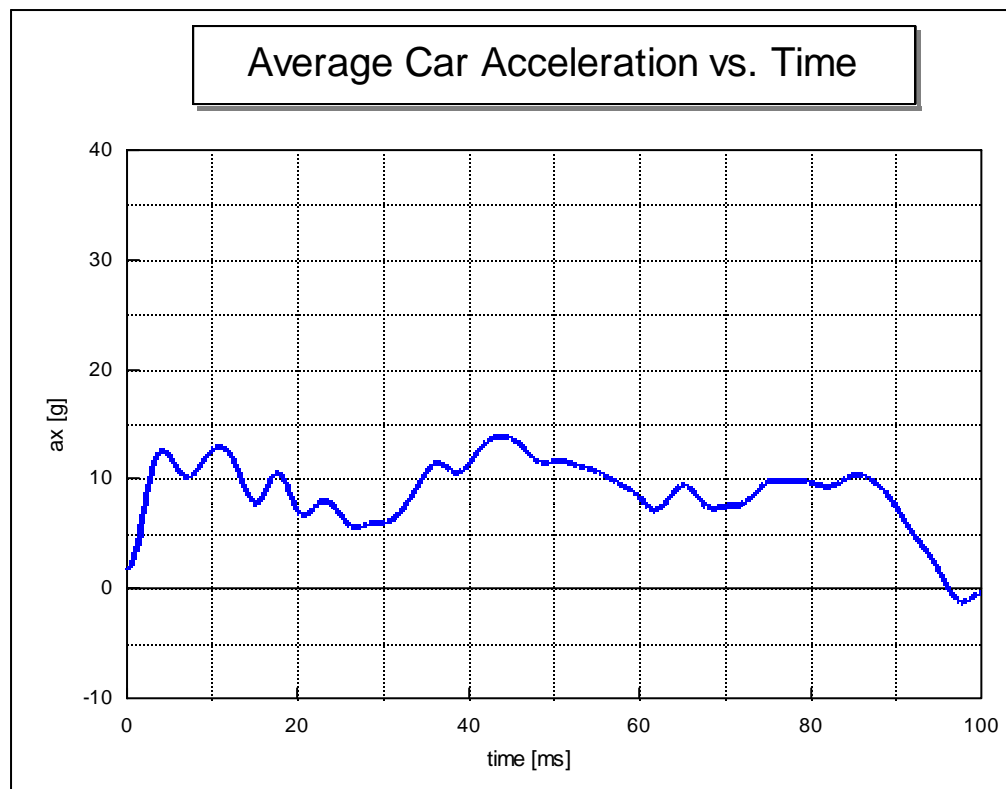


Figure 6.3.3-6 Rear Crash Acceleration vs. Time

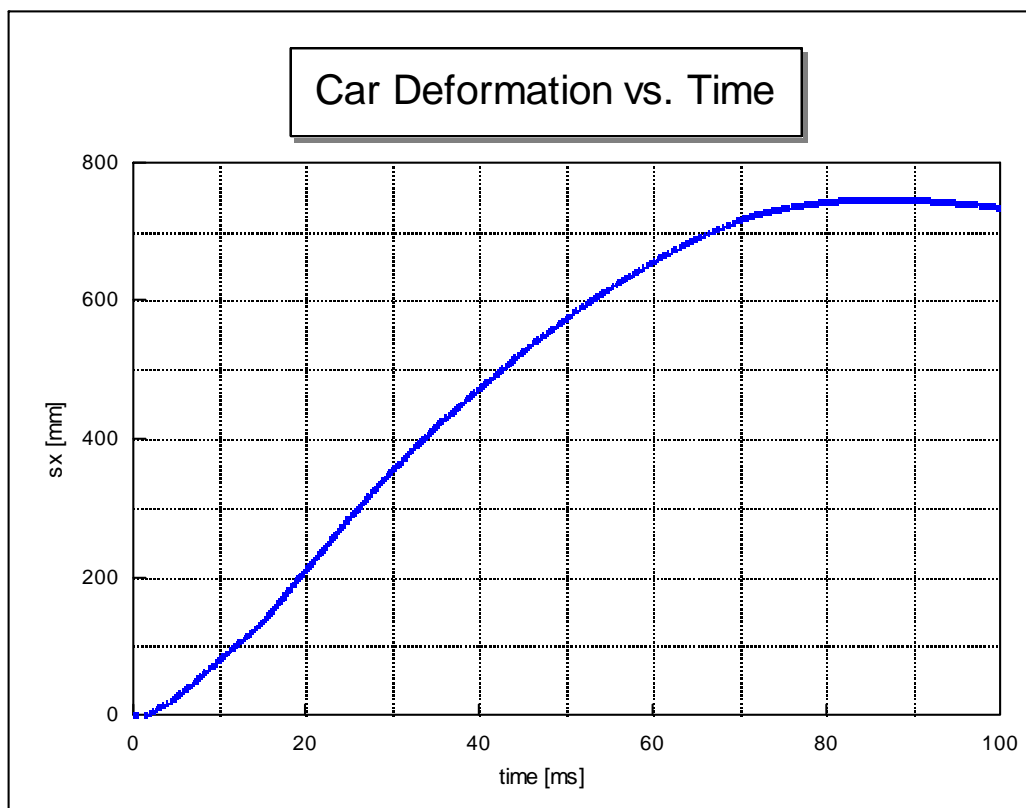


Figure 6.3.3-7 Rear Crash Deformation vs. Time

The following table (Fig. 6.3.3-8) explains the rear crash events after impact:

Time (ms)	Rear Crash
4.00	Initial folding of longitudinals rear
20.00	Spare tire contacts barrier
35.00	First buckling of crossmember rear suspension
40.00	Spare tire hits crossmember rear suspension
44.00	Buckling of the crossmember rear suspension
48.00	Buckling of the rear end rocker at the connection to longitudinal rear
52.00	Collapse of crossmember rear suspension
56.00	Buckling of the front end longitudinal rear
86.00	Maximum dynamic deformation reached

Figure 6.3.3-8 Rear Crash Events

This analysis shows that the structural integrity of the fuel tank and fuel filler was maintained during the event, so no fuel leakage is expected. The spare tire tub rides up during impact, avoiding contact with the tank.

Rear passenger compartment intrusion was restricted to the rear most portion of the passenger compartment, largely in the area behind rear seat. This result is due to good progressive crush exhibited by the rear rail.

6.3.4. Side Impact Analysis

The conditions for the side impact analysis are based on a European Side Moving Barrier Test. The European test specifically addresses injury criterion based on displacement data gathered from EUROSID side impact crash dummies. Automotive companies also include post-crash structural integrity and passenger compartment as additional requirements for this test.

The actual European side moving barrier uses a segmented deformable face which complies with a required set of different load versus displacement characteristics and geometric shape and size requirements. The barrier used in the analysis (Fig. 6.3.4-1) conformed to the geometric requirements (i.e., ground clearance, height, width, bumper depth). The European specification requires the impacting barrier to have a mass of 950 kg, making contact at ninety degrees relative to the vehicle longitudinal axis. The center line of the barrier is aligned longitudinally with the front passenger 'R-point'. The R-point is a car specific point which is defined by the seat/passenger location. The velocity of the side moving barrier at time of impact is designated to be 50 km/h.

Because the scope of analysis did not include side impact dummies, injury assessment could not be made. Injury performance is greatly affected by interior trim panel and foam absorber design as well as by structural crush. Evaluation of passenger compartment intrusion can be made by looking at door and B-pillar displacements and intrusion velocities. Structural integrity can be assessed by looking at the overall shape of the deformation, including any gross buckling of the B-pillar, rotation of the rocker rails, crush of the front body hinge pillar, folding of the door beams and door belts, and cross-car underbody parts such as the seat attachment members and the rear suspension cross member.

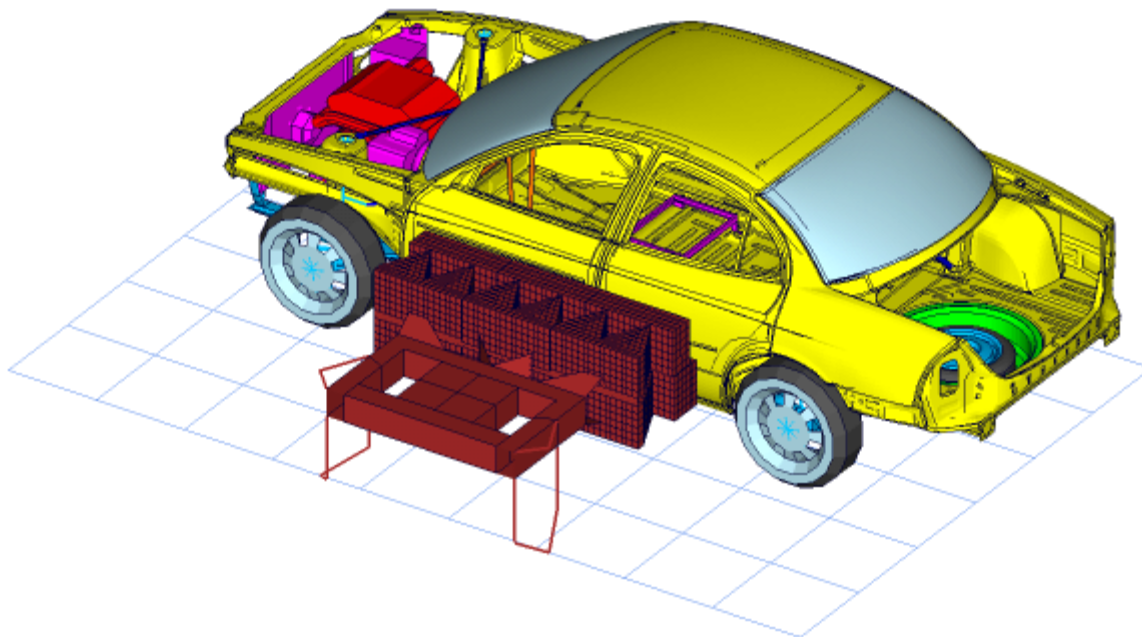


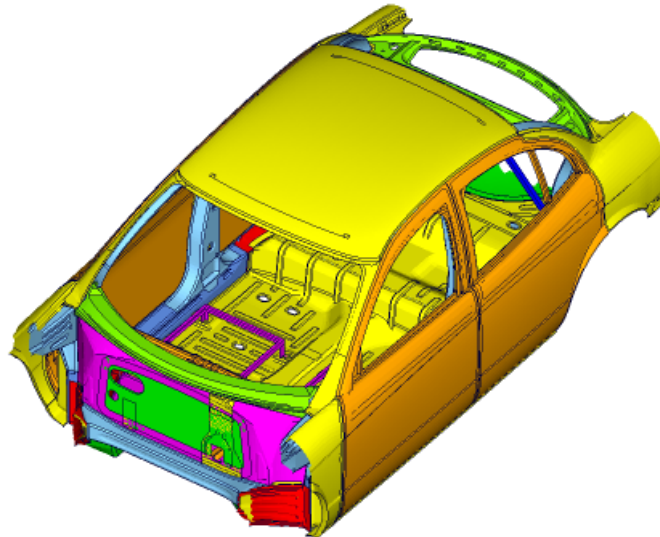
Figure 6.3.4-1 Side Impact Crash Analysis Setup

The side impact undeformed and deformed shapes are shown in Fig. 6.3.4-2 and 6.3.4-3, with the deformed shapes shown after 80 ms of impact.

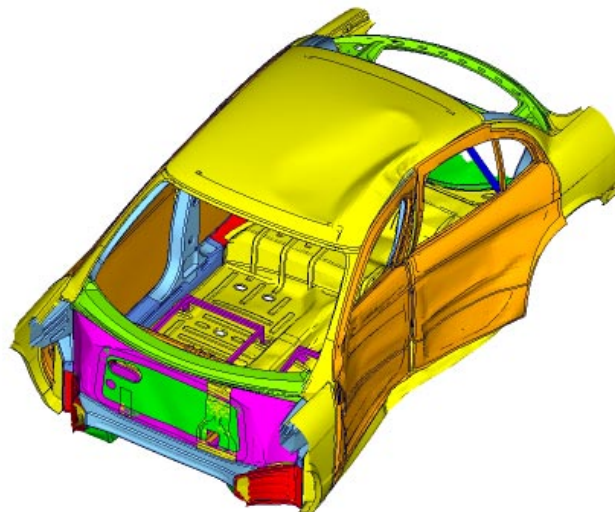
During the early stage of the impact, the outer door structure crushes, the B-pillar is stable. As the impact progresses the rocker starts to buckle and causes also a bulging of the floor section. At about 30 ms, the still stable structure of the B-pillar is moved by the barrier inside the car and therefore the roof starts to bulge. After 40 ms the B-pillar develops an inward buckling. After about 64 ms the maximum dynamic deformation is reached.

For the injury performance, the intrusion velocities of the structural parts, which could come in contact with the passengers, are important. Figures 6.3.4-5 and 6.3.4-6 show the intrusion velocities of typical points at the inner front door panel (No. 238) and the B-pillar inner (No. 235) (Fig.6.3.4-4).

The following Figures 6.3.4-2 and 6.3.4-3 show the deformed shape of the side structure:



$t = 0 \text{ ms}$



$t = 80 \text{ ms}$

Figure 6.3.4-2 Side Impact Crash Deformed Shapes

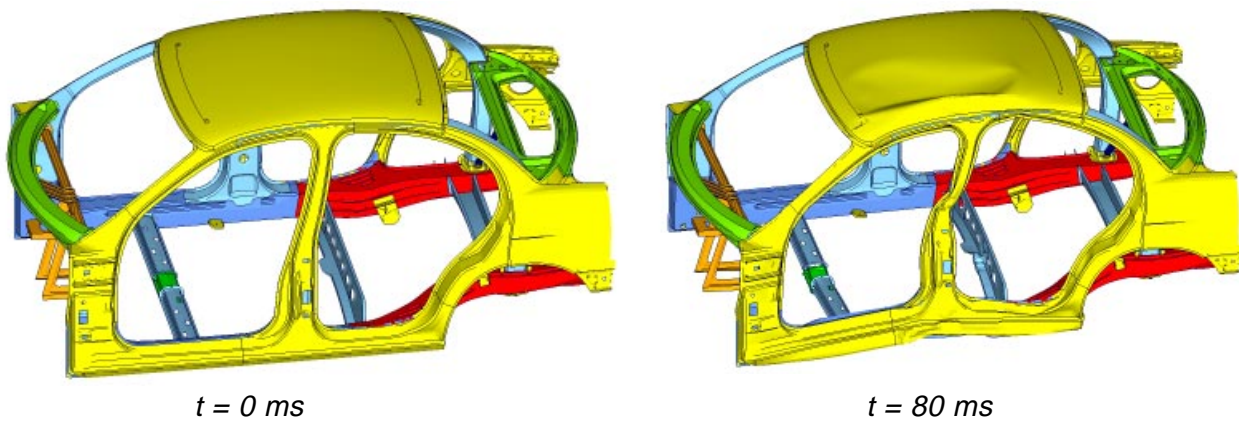


Figure 6.3.4-3 Side Impact Crash Deformed Shapes of Side Structure

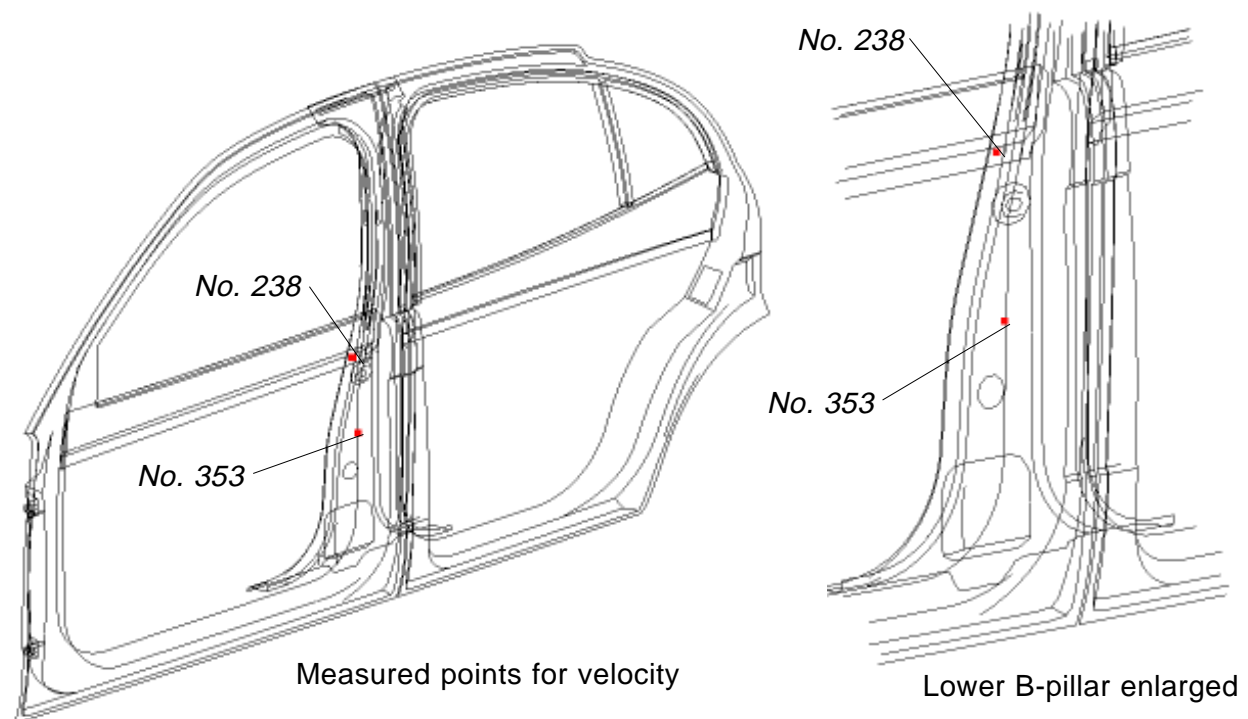


Figure 6.3.4-4 Side Impact Time History Node

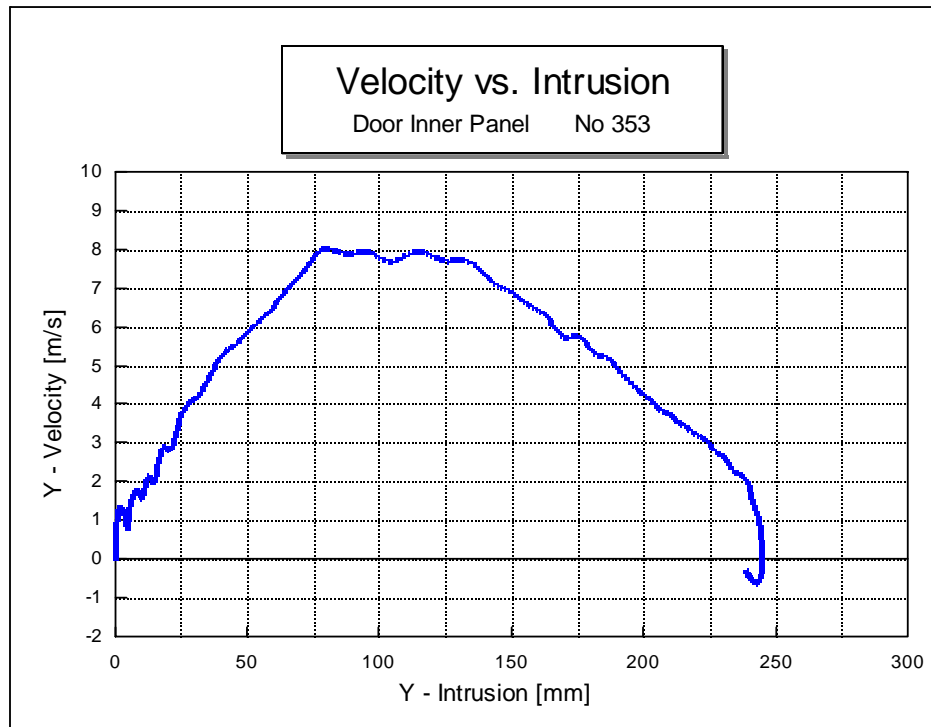


Figure 6.3.4-5 Side Impact Velocity vs. Intrusion at Node 353

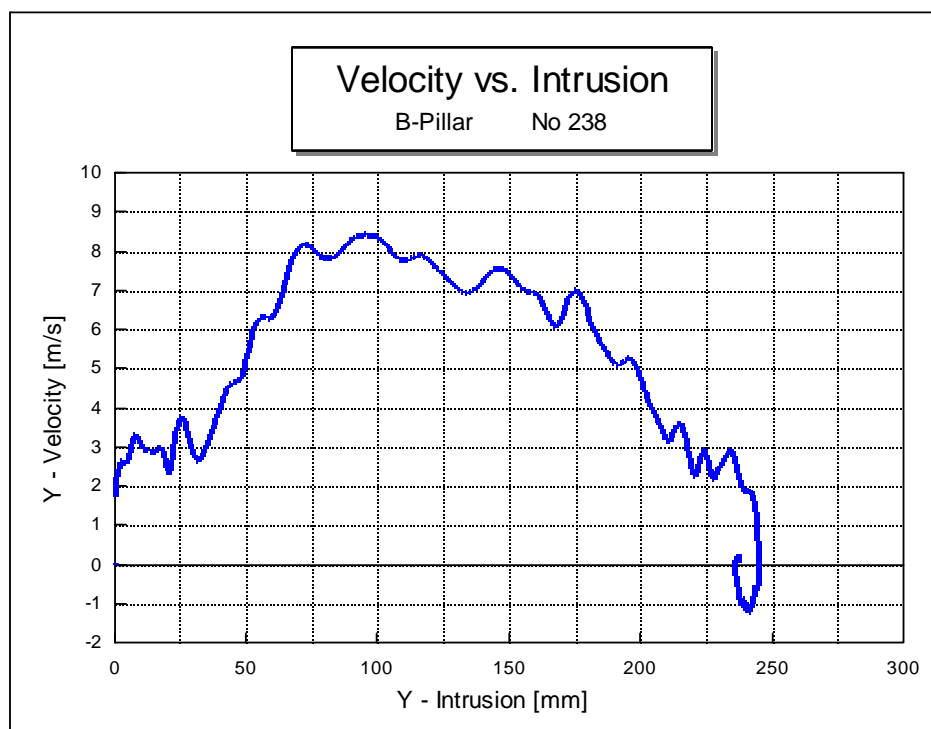


Figure 6.3.4-6 Side Impact Velocity vs. Intrusion at Node 238

The following table (Fig. 6.3.4-7) shows the side impact crash events:

Time (ms)	Side Impact
16.00	Buckling of the rocker in front of B-pillar
28.00	Buckling of the floor
35.00	Buckling of the roof
40.00	Buckling of the roof frame at the B-pillar
44.00	Buckling of the member kick up, still stable
48.00	Buckling of the brace tunnel
64.00	Maximum dynamic deformation reached

Figure 6.3.4-7 Side Impact Crash Events

The body side ring and doors maintained their integrity with only 248 mm of intrusion. The velocity of the intruding structure was tracked to determine the degree of injury an occupant may sustain. The maximum velocity was only 8 meters per second. The event is considered complete when the deformable barrier and vehicle reach the same velocity, in this case at 64 msec.

6.3.5. Roof Crush (FMVSS 216)

The conditions for the roof crush analysis are based on United States, FMVSS 216. This requirement is designed to protect the occupants in event of a rollover accident. The surface and angle of impact are chosen to represent the entire vehicle impacting the front corner of the roof.

The federal standard requires roof deformation to be limited to 127 mm (5 inches) of crush, and roof structure to support 1.5 times the vehicle curb mass or 5,000 lbs (22249 N), whichever is less.

For test purposes and repeatability, the complete body in white is assembled and clamped at the lower edge of rocker and the roof crush test is done in a quasi-static force versus displacement arrangement. In the computer analysis, the software program, LS-DYNA, requires that the roof crush be done in a dynamic, moving barrier description as compared to the quasi-static test.

Figure 6.3.5-1 shows the undeformed shape of the FE-Model used for the roof crush simulation. The shape of the structure after the limit of 127 mm deformation is shown in Figure 6.3.5-2.

The force versus displacement curve is shown in Fig 6.3.5-3. The peak force of 36150 N is reached after a deformation of 72 mm of roof crush. Based on the curb mass of 1350 kg, the crush force of 19865 N is required for the federal standards FMVSS 216. The analysis was continued to 127 mm (5 inches) of deflection in order to determine the ability of the roof to sustain the peak load past 72 mm of crush. The analysis shows that the roof meets the peak load requirements and is steady and predictable.

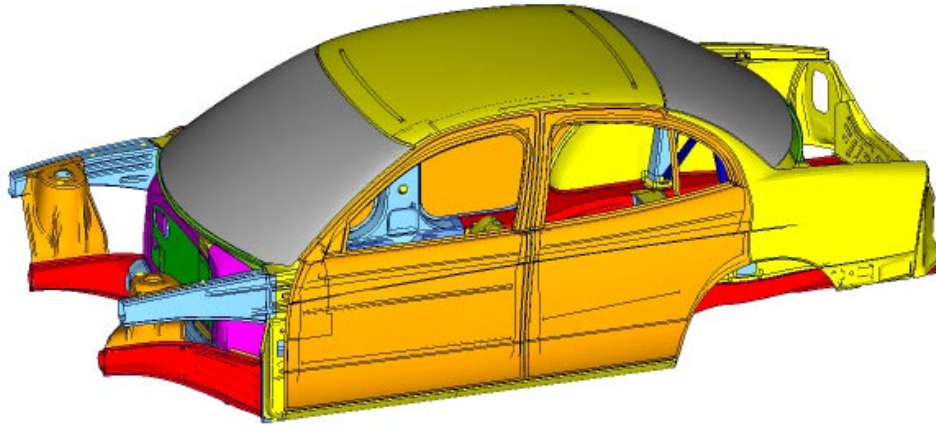


Figure 6.3.5-1 Roof Crush Undeformed Shape

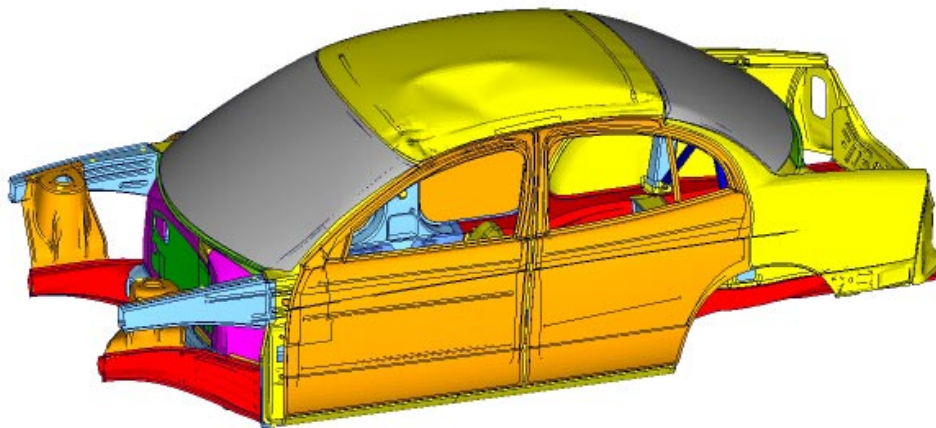


Figure 6.3.5-2 Roof Crush Deformed Shape

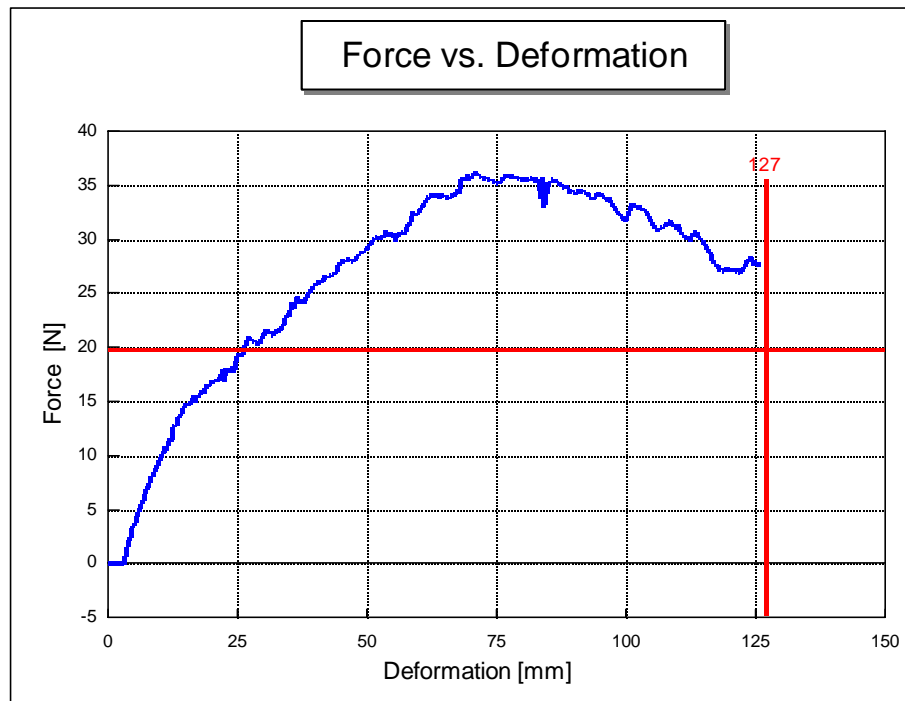


Figure 6.3.5-3 Roof Crush Deformation vs. Force

Analysis showed that 22.25 kN was reached within 30 mm of crush. The structure resisted the applied load all the way up its peak of 36.15 kN and continued to maintain it quite well even after peak, when it dropped to about 28 kN at 127 mm. The load was well distributed through the A, B and C-pillars and down into the rear rail.

6.4. CAE Analysis Summary

For the AMS Offset crash test the overall deformation and intrusion are the critical figures. For the NCAP crash test, the critical figure is the vehicle crash pulse. The target for the offset crash was to achieve low footwell intrusion. It is important to achieve a good balance between these two targets. The results of the crash analysis show that for the ULSAB a good compromise has been found to fulfill the AMS as well as the NCAP frontal crash, considering the dependencies between these two crash types.

To achieve the low footwell intrusion for the AMS crash a rigid front structure is needed. A rigid front structure, however, means higher acceleration in the NCAP

test and results in higher HIC (Head Injury Criteria) values for the passengers, with a maximum footwell intrusion of 149 mm for the AMS Offset crash and a maximum acceleration of 30.4 g for the NCAP crash, the ULSAB structure shows a good balance in these criteria. The results also document the high safety standards of ULSAB, especially if one considers that the NCAP crash analysis was run at 5 miles above the required speed of 30 mph and 36% more energy had to be absorbed.

The rear crash test requirements are addressing the fuel system integrity and low deformation in the rear seat area. The analysis shows no collapse of the surrounding structure of the fuel tank, contact with the fuel tank itself or the fuel filler routing. Considering the fact that there was no rear seat structure the analysis also shows a low deformation of the rear floor. For the rear crash analysis in the ULSAB program, the requirement was raised from 30 mph to 35 mph velocity of the rear moving barrier, resulting in an increase of 36% of its kinetic energy.

In the side impact crash test, good performance means acceptable intrusion of the side structure at low intrusion velocity. For both criteria the ULSAB achieved satisfactory results. The analysis shows a maximum intrusion of 250 mm and an intrusion velocity of 8 m/s at the inner door panel and the B-pillar. It is assumed that in a fully equipped car the intrusion will be even lower.

For the roof crush test the Federal standard requires the roof deformation to be limited to 127 mm of crush and the structure to support 1.5 times the curb mass or 5000 pounds, whichever is less. The force requirement of 19500 N was already met at 27 mm of crush. The continued analysis showed that the structure is steady and peak load of 36 kN was met after 72 mm of crush. This result confirms the role the side roof rail plays as important part of the ULSAB structure.

The ULSAB crash analysis has shown that reducing the body structure mass using high strength steel, in various grades and in applications such as tailor welded blanks combined with the applied joining technologies in the assembly, such as laser welding, does not sacrifice safety.

The goal was to maintain the high standards of state-of-the-art crash requirements, without compromising the ULSAB program goal to significantly reduce the body structure mass. The crash analysis of the ULSAB supports that this goal is reached.